DR. SHILONG PIAO (Orcid ID : 0000-0001-8057-2292)
DR. XUHUI WANG (Orcid ID : 0000-0003-0818-9816)

Article type : Opinion

Interannual variations of terrestrial carbon cycle: issues and perspectives

Shilong Piao[1,2,3*], Xuhui Wang[1], Kai Wang[1], Xiangyi Li[1], Ana Bastos[4], Josep G. Canadell[5], Philippe Ciais[1,6], Pierre Friedlingstein[7], Stephen Sitch[8]

[1] Sino-French Institute for Earth System Science, College of Urban and Environmental Sciences, Peking University, Beijing 100871, China.
[2] Key Laboratory of Alpine Ecology and Biodiversity, Institute of Tibetan Plateau Research, Chinese Academy of Sciences, Beijing 100085, China.
[3] Center for Excellence in Tibetan Earth Science, Chinese Academy of Sciences, Beijing 100085, China.
[4] Department of Geography, Ludwig-Maximilians Universität, Luisenstr. 37, 80333, Munchen, Germany.
[5] Global Carbon Project, CSIRO Oceans and Atmosphere, Canberra, ACT 2601, Australia
[6] Laboratoire des Sciences du Climat et de l'Environnement, CEA CNRS UVSQ, Gif-sur-Yvette 91191, France.
[7] College of Engineering, Mathematics and Physical Sciences, University of Exeter, Exeter EX4 4QF, UK.
[8] College of Life and Environmental Sciences, University of Exeter, Exeter EX4 4RJ, UK.

* Correspondence should be addressed to Shilong Piao (slpiao@pku.edu.cn)

This article has been accepted for publication and undergone full peer review but has not been through the copyediting, typesetting, pagination and proofreading process, which may lead to differences between this version and the Version of Record. Please cite this article as doi: 10.1111/GCB.14884

Abstract

With accumulation of carbon cycle observations and model developments over the past decades, exploring interannual variations (IAV) of terrestrial carbon cycle offers the opportunity to better understand climate-carbon cycle relationships. However, despite growing research interest, uncertainties remain on some fundamental issues, such as the contributions of different regions, constituent fluxes and climatic factors to carbon cycle IAV. Here, we overviewed the literature on carbon cycle IAV about current understanding of these issues. Observations and models of the carbon cycle unanimously show the dominance of tropical land ecosystems to the signal of global carbon cycle IAV, where tropical semi-arid ecosystems contribute as much as the combination of all other tropical ecosystems. Vegetation photosynthesis contributes more than ecosystem respiration to IAV of the global net land carbon flux, but large uncertainties remain on the contribution of fires and other disturbance fluxes. Climatic variations are the major driver to the IAV of net land carbon flux. Although debate remains on whether the dominant driver is temperature or moisture variability, their interaction, i.e. the dependence of carbon cycle sensitivity to temperature on moisture conditions, is emerging as key regulators of the carbon cycle IAV. On time-scales from the interannual to the centennial, global carbon cycle variability will be increasingly contributed by northern land ecosystems and oceans. Therefore, both improving Earth system models (ESMs) with the progressive understanding on the fast processes manifested at interannual time-scale and expanding carbon cycle observations at broader spatial and longer temporal scales are critical to better prediction on evolution of the carbon-climate system.

Introduction

Terrestrial ecosystems are the largest sink of airborne CO_2, offsetting more than one fourth of fossil fuel emissions (Le Quéré et al., 2018). This carbon sink has significantly slowed down global warming (Shevliakova et al., 2013). However, the land carbon sink is also by far the most uncertain component of the global carbon budget (Ballantyne et al., 2012; Keenan et al., 2018). The net land carbon flux is often deduced from the mass balance as a residual between fossil fuel emissions, atmospheric accumulation and ocean uptake, and exhibits large year-to-year differences, ranging from a net uptake of 4.0 PgC yr^{-1} to a net emission of 0.3 PgC yr^{-1} during the decade of the 1990s, exemplifying the variability of terrestrial carbon cycle.

The large IAV, on the one hand, complicates the detection of longer-term changes in the carbon cycle (Keeling et al., 1995). On the other hand, since the IAV of the global net land carbon flux is driven by climatic variations (Braswell et al., 1997; Zeng et al., 2005; Raupach et al., 2008; Liu et al., 2017), it provides a unique opportunity to observe the behavior of global terrestrial ecosystems exposed to climate anomalies, which cannot be achieved by any local observation or ecosystem manipulative experiment. The sensitivity of net land carbon flux to climatic variations was also used to provide an emergent constraint to future carbon cycle climate feedbacks (Cox et al., 2008; Cox et al., 2013). Therefore, IAV of the land carbon cycle is not merely characterizing terrestrial ecosystems, but also provides a “natural experiments” that help us better understand the complex relationships between climate and the terrestrial carbon cycle.

While IAV of terrestrial carbon cycle has received increasing research interest, debates remain about which regions and mechanisms underpin it. The prospects of using carbon cycle IAV to constrain carbon cycle climate feedbacks are also appealing. At the 25-year milestone of *Global Change Biology*, and with six decades of atmospheric CO_2 records, satellite records for four decades, rapidly growing ground-based observations networks and the development of global gridded land carbon cycle models by many research teams, it is time to review recent knowledge on the topic, shedding light on the projection of interactions between carbon cycle and climate at scales from the interannual to the centennial. In this review, we first discussed concept and methods to obtain IAV of terrestrial carbon cycle from the observation and modelling data. We then estimate the contribution of different regions, constituent fluxes and climatic factors to IAV, based on multiple observation data-streams and model results. We last discuss the perspective of utilizing information obtained from IAV to inform future projections of the carbon cycle response to climate change.

Separating IAV from seasonal variability and longer-term trends

The large year-to-year variability is a prominent characteristic of atmospheric CO_2 growth rate and net land carbon flux (Le Quéré et al., 2018). The first evidence of IAV in the atmospheric CO_2 growth rate was given by Keeling et al. (1976) and Bacastow (1976). For a few decades, atmospheric CO_2 concentration from few atmospheric stations and its ^{13}C isotopic signature were the only tool to attribute global carbon cycle IAV to land vs. ocean fluxes (Keeling et al., 1995). Since the 1980s, observation and modelling capacity have grown rapidly (Ciais et al., 2014). For example, we now have continuous atmospheric CO_2 measurements for six decades (Keeling et al., 1976), global atmospheric column CO_2 measurements from several satellites with data availability varying from a few years to a decade (e.g. Kuze et al., 2009; Eldering et al., 2017; Liu et al., 2018), more than 2000 eddy-covariance sites with varying operational period (Urbanski et al., 2007; Froelich et al., 2015; Aubinet et al., 2018; Burba, 2019). Atmospheric inversions use atmospheric CO_2 observations with atmospheric transport models to produce maps of surface fluxes, and their results now cover up to four decades (Rödenbeck et al., 2003; Chevallier et al., 2010; Le Quéré et al., 2018). Data-driven models upscale local eddy covariance data in space and time using gridded satellite and climate fields e.g. with machine learning algorithms (Tramontana et al., 2016), estimating land CO_2 fluxes for past four decades. On the process modelling side, gridded land carbon cycle models have been developed that encapsulate equations describing carbon, water and energy cycles, some further simulating carbon-nutrient interactions. For example, the TRENDY ensemble of 16 global land carbon cycle models following the same simulation protocol produced gridded land CO_2 fluxes for the annual update of the global carbon budget since 1960s (Le Quéré et al., 2018). These developments have brewed a growing body of literature on IAV in the global carbon cycle. Our perspective here is based on these papers and data-streams (see Table S1 for full list of datasets and models included). It should be noted that ground-based inventory of carbon stock change is an essential tool in assessing the long-term magnitude of carbon storage change (e.g. Pan et al., 2011), but seldom helpful in exploring IAV, because soil carbon stock change cannot be detected on a year-to-year basis (Smith, 2004) and systematic inventory surveys at country scale are usually performed in 5-10 year intervals (FAO-FRA, 2010).

An important concept to clarify is that IAV is a temporal component of the time series for carbon fluxes or climatic variables that is in addition to variability on shorter and longer time scales. For data/modelling time-series of several decades, IAV can be separated from seasonal variability and decadal and long-term trends. When annual data were analyzed, detrended anomalies were commonly obtained as IAV (e.g. Anderegg et al., 2015). But, when monthly or higher resolution data were analyzed, there are different methods in the literature to extract the IAV signal from other modes of variability. Different methods may yield different results, especially for time series with high temporal resolutions (e.g. monthly or daily). To illustrate this point, we compare six different methods for extracting IAV from monthly CO_2 growth rates at Mauna Loa (MLO): Fast Fourier Transform (FFT; Rödenbeck et al., 2018), Singular Spectrum Analysis (SSA; Mahecha et al., 2010), Ensemble Empirical Mode Decomposition (EEMD; Hawinkel et al., 2015), detrended annual growth rate with no filter (SMN; Wang et al., 2014c), detrended annual growth rate with a 6-month smoothing filter (SMS; Patra et al., 2005) and with a 13-month smoothing (SML; Wang et al., 2013). In frequency-based methods (FFT, SSA and EEMD), we can define IAV as the sum of all frequency components with frequencies between 2 years and 11 years, while in the three other methods (SMN, SMS and SML), IAV contains all residual variability from the mean seasonal cycle and the long-term trends. The magnitude of IAV of CO_2 growth rate (i.e. standard deviation of extracted IAV) during 1959-2017 varies between the different methods from 0.9 PgC yr^{-1} to 2.5 PgC yr^{-1} (Figure 1), with four of the six methods resulting in a magnitude of between

1.0 and 1.4 PgC yr^{-1} (Figure 1). Overall, five of the six methods extracted similar signals of IAV time series, except for EEMD (Figure 1b) that produced the magnitude of IAV larger by a factor of two. IAV from EEMD contains mixture of signals from different temporal scales, indicating that this method is less suitable for isolating IAV, though it may work well for trend analyses with shorter time series (Chen et al., 2017). The lower magnitude of IAV from SMS and SML compared with FFT and SSA, suggests that the subjective choices with lower-pass filters probably removes some IAV signals (Figure 1a). Nevertheless, irrespective of the methods used to isolate it, IAV is a significant temporal component of the global carbon cycle variability (Baldocchi et al., 2016; Zhang et al., 2018), which has larger magnitude of variance than longer-term trends (Figure 1a).

Tropical semi-arid regions are hotspots for IAV of global net land carbon flux

At the time of 1970s, interannual variations of ocean carbon uptake were thought to be chiefly responsible for IAV of atmospheric CO_2 growth rates (Keeling et al., 1976; Bacastow, 1976). This view slowly changed towards a land dominance. Byy the same year when *Global Change Biology* was launched, Keeling et al. (1995) used CO_2 and ^{13}C measurements from SCRIPPS-CIO network and a global box carbon cycle model to identify a significant land contribution to IAV of atmospheric CO_2 growth rate, though uncertainty in fractionations and box carbon cycle models precluded the conclusion of land/ocean dominance at the time (e.g. Francey et al., 1995).In the early 2000s, analyses of ^{13}C isotopic measurements (Keeling et al., 2005; Rayner et al., 2008), 3D atmospheric inversions (Bousquet et al., 2000; Gurney et al., 2008; Roedenbeck 2003) and land carbon cycle models (Zeng et al., 2005) independently confirmed the dominance of IAV being from terrestrial ecosystems (Figure 2). The diversity and heterogeneity of terrestrial ecosystems make it challenging to accurately identify the dominant land regions contributing to global land carbon cycle IAV. Both northern hemisphere and tropical terrestrial ecosystems were reported to be responsible for years showing anomalous large atmospheric CO_2 growth rate (e.g. Ciais et al., 2005; Jones & Cox, 2005; van der Werf et al., 2004; Knorr et al., 2007; Gatti et al., 2014).

Studies based on the eddy-covariance data-driven model (FLUXCOM with both remote sensing and climate data as forcing dataset; Tramontana et al., 2016; Jung et al., 2019) and atmospheric inversions (Table S1) ubiquitously attribute most of global IAV to tropical land ecosystems since 1980s (e.g. Bousquet et al., 2000; Patra et al., 2005; Baker et al., 2006; Rayner et al., 2008; Jung et al., 2011, 2017; Peylin et al., 2013; Rödenbeck et al., 2018), though the absolute magnitude of IAV in FLUXCOM data is about one order of magnitude smaller than the other approaches (Figure 3a; Figure S2). Studies also differ on the ecosystems which IAV sourced from. Some inversions show higher variability over the moist tropical forest region (Marcolla et al., 2017), while process-based carbon cycle models challenged this view by suggesting that the less productive but extensive semi-arid ecosystems up to 45^{o}N have the greatest contribution to IAV of net land carbon flux (Ahlström et al., 2015). Recent satellite-based biomass carbon stock change also implies a relative stronger role of tropical semi-arid ecosystems than forests in driving IAV of net land carbon flux (Fan et al., 2019). It appears counter intuitive at first sight that the less productive semi-arid lands could contribute more to IAV than wet forests where a small change in the balance between large and opposite CO_2 fluxes of photosynthesis and respiration (Wang et al. 2013) could lead to a large change in the net flux. On the other hand, semi-arid ecosystems can become a large carbon sink in a wet year because vegetation productivity was found to be enhanced (Poulter et al., 2014) and those systems contain less soil carbon as a substrate for soil respiration anomalies. This positive carbon sink anomaly can be amplified by the "memory" effect of previous droughts, because previous droughts can reduce the current size of biomass and litter, which acts to suppress respiration (Poulter et al., 2014). However, it was not yet mature to conclude the issue because the findings of Ahlström et al. (2015) were mainly based on land carbon cycle models, and these models are known to have issues, for example, in reproducing the timing of events that cause large year-to-year variability (Keenan et al., 2012). Satellite-based CO_2 inversions, as well as satellite-based biomass carbon stock change, provide an potential alternative source of information on spatial pattern of IAV, but they are at the moment only available for few years (Palmer et al., 2019; Fan et al. ,2019).

Revisiting here this issue following the land cover classification (Figure S1) and methods in calculating regional contribution by Ahlstrom et al. (2015), but using the latest results from land carbon cycle models, global atmospheric inversions based on in-situ data, and eddy-covariance data-driven model (FLUXCOM) (Table S1), we found that the share in contributions of tropical semi-arid ecosystem versus tropical non-semi-arid ecosystem to global IAV between different approaches is in fact quantitatively not so different (Figure 3). In land carbon cycle models the contribution of semi-arid tropical ecosystems to IAV of global net land carbon flux (35% - 47%) is marginally larger than the contribution of non-semi-arid tropical ecosystems (33% - 38%) during 1980-2016. The FLUXCOM data-driven model shows similar contribution to IAV of global net land carbon flux from tropical semi-arid ecosystems and tropical non-semi-arid ecosystems (Figure 3b). Semi-arid ecosystems outside the tropics (>30°N or <30°S), however, account for less than 2% of IAV of global net land carbon flux in all data-streams (Figure 3b), and are not necessarily more variable than forests of the same region (Shiga et al., 2018). In the climate space, a higher mean annual temperature seems a better predictor of IAV than aridity, here defined by the mean annual water deficit (precipitation minus potential evapotranspiration) (Figure 3c).

When comparing different approaches, the contribution to global IAV from the extra-tropics (e.g. Europe; Figure 3a) is relatively larger in atmospheric inversions than in other approaches. This may be because surface in-situ atmospheric CO_2 observations are sparse over the tropics (Gaubert et al., 2018), limiting the inversions' capability to separate IAV from the tropics and from the extra-tropics (Peylin et al., 2013), regardless of the improving nominal spatial resolution of the atmospheric inversions (Chevallier et al., 2010; Le Quéré et al., 2018). The recent developments of satellite-based CO_2 inversions, with coverage of tropical continents being as dense as that of northern lands, however, have the potential to better resolve the issue (e.g. Liu et al., 2017; Palmer et al., 2019) though uncertainties remain large at the moment (Houweling et al., 2015; Crowell et al., 2018).

Photosynthesis carbon uptake contributes more to IAV than ecosystem respiration

Photosynthesis (GPP) and ecosystem respiration (TER) are the two largest constituent carbon fluxes that mostly determine the IAV of net land carbon flux (Houghton, 2000; Van der Werf et al., 2010). The hotspot regions for IAV of net land carbon flux are generally coincident with those of GPP and TER (Jung et al., 2011). Both land carbon cycle models and FLUXCOM generally agree that, globally, IAV of GPP largely drives IAV of net land carbon flux (as indicated by the blue shading in Figure 4b and c; Jung et al., 2011; Ahlström et al., 2015). However, the estimated contribution of GPP IAV to the net carbon balance IAV varies from 56% to more than 90% among land carbon cycle models (Ahlström et al., 2015). In over 72% of the FLUXNET sites (Table S1) with more than 5 years of observations, GPP IAV has a larger contribution than TER IAV to the IAV of net land carbon flux (Figure 4d; e.g. Wu et al., 2012; Jensen et al., 2017; Marcolla et al., 2017; Baldocchi et al., 2018), since GPP is more sensitive to climatic variations interannually (e.g. Schwalm et al., 2010; Shi et al., 2014; Kim et al., 2016). Large uncertainties remain on the spatial patterns of the relative contribution of vegetation productivity and respiration fluxes to IAV of net land carbon flux (Figure 4b-d; e.g. Ciais et al., 2009; Piao et al., 2009; Ahlström et al., 2015; Jung et al., 2017; Liu et al., 2018).

Fire emissions can explain a significant proportion of regional anomalies of the net land carbon flux in the tropics during specific extreme years, mainly peat fires in Indonesia in 1997/1998 (Van der Werf et al., 2004) and droughts in the Amazon basin in 2010 and 2015 (Gatti et al., 2014; Aragão et al., 2018). African savannas that have large contribution to the mean fire emissions show small fire emission IAV (van der Werf et al., 2017), which can be understood as these systems 'will always burn' during the dry season. The variations of carbon emissions due to fire (Van der Werf et al., 2017) are strongly correlated with CGR over the past two decades (R^2=0.46, P<0.01, Figure 2), however, their magnitude (0.23 PgC yr^{-1}) accounts for less than one third of the IAV in net land carbon flux estimated by atmospheric inversions. Note that this number does not account for the legacy effects of fire on depleted soil carbon for respiration and stimulated/reduced post-fire productivity. Tree mortality induced by drought events may significantly affect the net land carbon flux of tropical forests, contributing largely to carbon flux anomalies during the dry years 2005 and 2010 over the Amazon (Phillips et al., 2009; Da Costa et al., 2010; Moser et al., 2014). The effect of tree mortality may last quite a few years after the drought events (Saatchi et al., 2013; Anderegg et al., 2015; Yang et al., 2018). Still, no evidence suggests tree mortality as a significant factor to IAV of global net land carbon flux at the moment, because both land carbon cycle models and data-driven models (e.g. FLUXCOM) have not yet well represented forest mortality process. With the expectation of increasing drought frequencies in the tropics (IPCC, 2012; Sillmann et al., 2013), the role of tree mortality and associated disturbances such as pests and diseases may become more obvious in the future (Lewis et al., 2015).

Carbon emissions from fossil fuel combustion are large in magnitude but have relatively small IAV at global scale (s.d. of 0.37 PgC yr^{-1}, R^2=0.01, P=0.55). Fossil fuel IAV thus cannot account much for the large year-to-year variations in atmospheric CO_2 growth rate (Figure 2; Langenfelds et al., 2002). Land use change flux estimated by bookkeeping models has even smaller magnitude of IAV (s.d. of 0.14 PgC yr^{-1}, R^2<0.01, P=0.96) (Figure 2; Hansis et al., 2015; Houghton and Nassikas, 2016), which is probably due to the 5-yr time-scale of the underlying forcing data and the fact that bookkeeping models do not consider IAV of climate affecting the components of land use change flux. Still, large uncertainties exist in the land use change flux estimates and therefore their role in IAV. For example, whether the IAV in the carbon sink over plantations and re-growing secondary forests should be accounted as IAV of land use change flux remains inconsistent across studies (Houghton et al., 2010; Pongratz et al., 2014; Arneth et al., 2017; Le Quéré et al., 2018).

Climatic drivers of carbon cycle IAV: temperature, precipitation and their interactions

The largest anomaly of atmospheric CO_2 growth rate over the instrumental records is in year 1992 (Figure 2). The approximately negative -2 PgC yr^{-1} anomaly (Tans & Keeling, 2019) is associated with the volcanic eruption in Mount Pinatubo in June 1991 (Le Quéré et al., 2018). Earth observations were pretty much nascent at that time, rendering the spatial pattern of the net land carbon flux anomaly largely uncertain (Figure 5; Baker et al., 2006; Brovkin et al., 2010). The mechanisms driving the large carbon sink after Pinatubo eruption is still not fully understood, since the latest land carbon cycle model ensemble cannot capture the post-Pinatubo land sink anomalies (Le Quéré et al., 2018). On the one hand, the volcanic-aerosol induced increase of diffuse light fraction can enhance photosynthesis (Roderick et al., 2001; Gu et al., 2003), while, on the other hand, the volcanic induced surface cooling could also suppress the heterotrophic respiration and biomass burning (Lucht et al., 2002; Angert et al., 2004). Most models do not account both processes at the same time. The one land carbon cycle model that does estimated that both mechanisms contribute ~1 PgC respectively to global land sink anomaly in 1992 (Mercado et al., 2009).

Except for few large volcanic eruptions, El Niño Southern Oscillation is the major climatic mode that alters global temperature, precipitation and solar radiation (Gu and Adler, 2011), and thus drives IAV of the carbon cycle (Bacastow, 1976; Keeling & Revelle, 1985; Rayner et al., 2008). The largest three El Niño events over past thirty years (1987, 1997 and 2015) led to average positive anomalies of net land carbon flux ranging from 0.22±0.16 PgC yr^{-1} by FLUXCOM (Tramontana et al., 2016) to 0.94±0.31 PgC yr^{-1} by atmospheric inversions (Le Quéré et al., 2018), while the largest three La Niña years (1989, 1999 and 2011) led to anomalies of carbon uptake from 0.21±0.13 PgC yr^{-1} by FLUXCOM (Tramontana et al., 2016) to 1.19±0.39 PgC yr^{-1} by land carbon cycle models (Sitch et al., 2015) (Figure 5). Hot and dry climate conditions in El Niño years are the primary reasons for the lower net carbon uptake or net carbon release by terrestrial ecosystems (Jones et al., 2001; Zeng et al., 2005; Piao et al., 2009), which is particularly evident in tropical ecosystems (Figure 5; Figure 6 b-d; Liu et al., 2017; Gloor et al., 2018).

Warmer temperature reduces tropical net carbon uptake (Wang et al., 2013; Schneising et al., 2014), which was found to be the dominant climatic driver in many studies of atmospheric CO_2 growth rate (Figure 6; Table 1) and tropical ecosystems (e.g. Kindermann et al., 1996; Clark et al., 2003; Doughty and Goulden, 2008). The negative impacts of higher temperature come from the reduced vegetation productivity and enhanced heterotrophic respiration over the tropics. Higher temperature was observed to reduce vegetation productivity over tropical ecosystems (Corlett et al., 2011; Clark et al., 2013; Aubry-Kientz et al., 2015) since their photosynthesis may operate at a temperature optimum close to current air temperature (Huang et al., 2019). Warming induced increase in vapor pressure deficit could also directly stress photosynthesis through reducing canopy conductance (Novick et al., 2016; Yuan et al., 2019). In addition, higher temperature was shown unanimously to increase heterotrophic respiration through enhanced microbial metabolism that decompose soil carbon (Wang et al., 2014b; Bond-Lamberty et al., 2018), though the temperature sensitivity remains uncertain and changing with time and carbon stock size (Mahecha et al., 2010; Crowther et al., 2016; Melillo et al., 2017).

Water availability is one of the major climatic variables that affect anomalies of tropical net carbon flux (e.g. Gatti et al., 2014; Jung et al., 2017). Anomalies of water availability, often proxied by precipitation, were found to be significantly correlated with anomalies of atmospheric CO_2 growth rate in several studies (Table 1) and also with net carbon flux of tropical ecosystems (Figure 6 b-d; Tan et al., 2013). The impacts of drought on ecosystem carbon cycling have been extensively studied, but its mechanisms are complex and incompletely understood (Corlett, 2016). Soil moisture deficit can directly induce stomatal closure (Manzoni et al., 2013) and reduce light use efficiency (Stocker et al., 2019). In addition, drought can inhibit new leaf formation and accelerate leaf-fall (Nepstad et al., 2002) leading to lower vegetation greenness (Xu et al., 2011; Anderson et al., 2018) and thus lower photosynthesis carbon uptake (Tan et al., 2013; Doughty et al., 2015). However, deep root system or altered allocation strategy could buffer drought impacts (Nepstad et al., 1994; Oliveira et al., 2005; Doughty et al., 2015), leading to debates on whether net primary production reduces in response to droughts (Moser et al., 2014; Doughty et al., 2015). Response of soil respiratory flux to drought is even less well understood, but recent studies show strong enhancement of soil CO_2 emission after severe drought events (O'Connell et al., 2018). Nevertheless, there is general agreement on drought-induced increasing mortality rates (e.g.

Philipps et al., 2009; de Costa et al., 2010; Brienne et al., 2015) and flammability (e.g. Aragão et al., 2008; Liu et al., 2017), which could substantially contribute to positive anomalies of net carbon flux in drought years (Gatti et al., 2014; van der Laan-Luijkx et al., 2015; Withey et al., 2018).

Despite growing understanding of the drivers and response of IAV of carbon fluxes, whether variations in thermal conditions contribute more than moisture conditions in driving IAV of the tropical net carbon flux (e.g. Wang et al., 2013; Schneising et al., 2014; Wang et al., 2014c), or the reverse (e.g. Wang et al., 2016; Jung et al., 2017; Humphrey et al., 2018), remains debated in the literature. At global/continental scale, interannual temperature anomalies consistently better explain IAV of atmospheric CO_2 growth rate and tropical net land carbon flux than interannual precipitation anomalies (Figure 6a), regardless of the approaches in estimating net land carbon flux. On the contrary, recent studies show that if replacing precipitation with other indices of water availability considering the balance of water supplies and demands, such as the Palmer Drought Severity Index (PDSI) and Terrestrial Water Storage (TWS; i.e. the sum of groundwater, soil moisture, snow, surface water, ice, and biomass (Tapley et al., 2004)), the correlation between IAV of CO_2 growth rate and water availability indices becomes stronger (Keppel-Aleks et al., 2014; Jung et al., 2017) and even surmounts the relationship between IAV of CO_2 growth rate and temperature, when using global and time-lagged anomaly of TWS (Humphrey et al., 2018). However, the stronger correlation between global TWS and the CO_2 growth rate as compared to the tropical TWS only (Humphrey et al., 2018) should be viewed with cautions, because it may be interpreted as a significant contribution of moisture limited northern ecosystems to IAV, which is inconsistent with the lower contribution of land fluxes of northern ecosystems to global IAV (Figure 3).

These lines of evidence highlight the challenge to separate the contributions of climatic factors to IAV of net land carbon flux: On the one hand, IAV in tropical temperature and precipitation are significantly negatively correlated (e.g. Gu and Adler, 2011; Zscheischler et al., 2014), making the separation of their respective contributions difficult. On the other hand, warmer temperature affects ecosystems not only through directly influencing metabolism but also indirectly through higher evaporative demand and increased VPD (Novick et al., 2016; Yuan et al., 2019) and interacts with insufficient precipitation supply to result in drought stress (Brando et al., 2014; Corlett, 2016). There is also growing evidence showing that photosynthesis and respiration are significantly affected by the interactions between temperature and moisture conditions (Zhou et al., 2016; Reich et al., 2018; Wang et al., 2018). However, only few studies on the relationship between IAV of CO_2 growth rate and climate considered the interactions of climatic factors (Table 1). To illustrate this point, we reanalyzed the relationship between IAV of climatic factors, reconstructed terrestrial water storage, leaf area index and CO_2 growth rate with the structural equation model (SEM) (Figure 7), which has been widely used to understand direct and indirect relationship among potential driving factors (Grace, 2006). Since variability of CO_2 growth rate is dominated by tropical land ecosystems (see Section 3), we aggregated gridded variables over the tropical region. The SEM results confirm the dominant role of temperature and TWS in driving IAV of CO_2 growth rate (e.g. Humphrey et al., 2018) and further demonstrate the need to consider interactions of climatic factors in predicting IAV of CO_2 growth rate. IAV of TWS is mostly explained by both precipitation and temperature anomalies (Figure 7), consistent with Gloor et al. (2018) who found strong negative correlation between tropical temperature and TWS anomalies. Thus, the indirect pathway of temperature impacts on CO_2 growth rate through interaction of temperature and precipitation has significant contribution to IAV of CO_2 growth rate (Figure 7), which also explains why water availability indices or soil moisture datasets considering evaporative demands have stronger predictive power to IAV of CO_2 growth rate than precipitation.

Sensitivities of atmospheric CO_2 growth rate to interannual tropical temperature variations (γ^{IAV}) were reported by many studies, whose results differ by a factor of two (Table 1). Different methods to isolate IAV signal in CO_2 growth rate time series (see Section 2) and different temperature data used could affect the derived magnitude of γ^{IAV}. Calculating γ^{IAV} based on tropical land and ocean surface temperature anomalies (e.g. Cox et al., 2013; Chylek et al., 2018) leads to higher value than calculation based on tropical land temperature anomalies (Table 1). The other major source leading to the differences is the time period used to derive γ^{IAV}. γ^{IAV} during 1960s-1970s was significantly lower than that during 1990s-2000s (Wang et al., 2014c; Rödenbeck et al., 2018). The magnitude of γ^{IAV} in the most recent two decades dropped down, though it is still larger than that during 1960s-1970s (Rödenbeck et al., 2018; Luo & Keenan, 2019). Changing γ^{IAV} can result either from geographical reasons, as temperature anomalies of the tropical region became more coherent over time (Yang et al., 2019), leading to expansion of the geographical area that have synchronous temperature-driven variations of net ecosystem carbon flux (Jung et al., 2017), or from a physiological response of tropical ecosystems becoming more sensitive to temperature variations under drier conditions (Wang et al., 2014c; Luo & Keenan, 2019), leading to increasing variability of CO_2 growth rate (Anderegg et al., 2015) under similar magnitude of temperature variability. The changing sensitivity of net land carbon flux to interannual temperature variations not only took place in the tropics, but also in the northern hemisphere, where positive temperature effects over IAV of net land carbon flux has been weakening over the past three decades (Piao et al., 2017; Yin et al., 2018; Wang et al., 2018). There is growing concern that these findings are early warning signals of driver shift or even abrupt status shift of the terrestrial ecosystem dynamics (Lewis et al., 2015; Peñuelas et al., 2017; Liptak et al., 2017).

Can we constrain future carbon cycle-climate feedbacks from carbon cycle IAV?

The prospect that using historical interannual carbon cycle variations to help constrain future land carbon cycle-climate feedback, known as γ^{LT} (see Friedlingstein et al. (2006) for detailed definition), at centennial scale (Cox et al., 2013) is of high interest to the carbon cycle community and of great policy relevance. γ^{LT} is one of the major sources of uncertainties in climate projections by ESMs (Friedlingstein et al., 2006; Arora et al., 2013) but not observable. Applying the emergent constraint approach, which builds on an empirical relationship between the measurable interannual sensitivity (γ^{IAV}) and γ^{LT} among ESMs, Cox et al. (2013) lower the best estimate of γ^{LT} by 23% and reduce projected uncertainty of γ^{LT} by 56%. This success has inspired growing studies on carbon cycle IAV and searching for other observable metrics to constrain future evolution of the global carbon cycle (Wenzel et al., 2014; Mystakidis et al., 2016; Liu et al., 2019).

However, there are concerns on efficiency and even validity of the emergent constraint on γ^{LT}. The efficiency of the emergent constraint relies largely on the existence and strength of a relationship between the measurable interannual sensitivity (γ^{IAV}) and the future long-term one (γ^{LT}) across ESMs, since error reductions come through replacing the original model spread of the long-term target projection with the propagated error of the measurable metric and the metric-target relationship across ESMs (Hall et al., 2019). Recent studies found that the metric-target relationship between γ^{IAV} and γ^{LT} is dependent on the selection of ESM ensemble and seasonal variants of the metric (Wang et al., 2014a; Keppel-Aleks et al., 2018), which could result in no error reduction on the future sensitivity through the emergent constrain (Wang et al., 2014a).

Moreover, statistically significant and physically meaningful relationship between γ^{IAV} and γ^{LT} is the premise for the validity of the emergent constraint, in order to avoid meaningless significant correlation by chance (Caldwell et al., 2014). The mechanistic links between γ^{IAV} and γ^{LT}, however, remain unclear. IAV of atmospheric CO_2 growth rate mainly brings information on "fast" processes controlling fluxes of photosynthesis and respiration of mainly tropical ecosystems (involving fast carbon pools such as plant reserves, fine roots, litter and labile soil carbon). With increasing time-scale from interannual to decadal and centennial, controlling regions and processes may change. According to the CMIP5 ESMs (Table S1), the tropical region contributes to 87% of net land carbon flux variance at interannual scale (Figure 8; see also section 3), but the northern hemisphere's extra-tropics contribute to 41% of net land carbon flux variance at centennial scale. Moreover, contribution of ocean carbon flux variations to total carbon flux variations increases from interannual scale to centennial scale (Figure 9), even though some ocean model may underestimate the decadal variability in ocean carbon flux (Rodenbeck et al., 2015; Le Quere et al., 2018). It is questionable whether climate sensitivity of tropical ecosystems may represent that of temperate ecosystems, given the differences in the historical relationship between net carbon flux and climatic variations (Figure 6b-d), as well as emerging role of ocean ecosystems (e.g. Randerson et al., 2015) at centennial scale (Figure 9). There are also slow-evolving and climate-sensitive processes and tipping elements, which may not manifest themselves on interannual time scales, but contribute to or even dominates the climate sensitivity of terrestrial ecosystems at the time scale of γ^{LT}, such as change in nutrient limitations, soil carbon turnover and permafrost thawing (Arneth et al., 2010; Zaehle et al., 2011; Zhang et al., 2011; Friend et al., 2014; Koven et al., 2015). There is a risk that a diagnostic inter-model relationship between γ^{IAV} and γ^{LT} depends on the model ensemble considered, due to similar carbon turnover parameterization or common deficiencies in process representations in ESMs, like widely under-representation of nutrient cycling, climate-induced mortality and permafrost dynamics (IPCC, 2013). Therefore, using γ^{IAV} to constraint γ^{LT} would possibly lead to underestimating the projected uncertainties of carbon cycle-climate feedbacks.

Conclusions

The IAV of the terrestrial carbon cycle represents an integrative research opportunity that has distinctive characteristics to seasonal variability and long-term trends. The IAV of global net land carbon flux was dominated by the tropical region, where semi-arid ecosystems may contribute as large as the sum of all the other tropical ecosystems. Climate perturbations, like volcanic eruptions, or variability of atmospheric circulation modes, drive carbon cycle variability through exposing ecosystems to year-to-year climatic variability. With growing numbers of observations, manipulation experiments and modelling capacities, the impacts of single climatic factors (e.g. temperature or precipitation) on IAV of net carbon flux became better understood, but interactive impacts of multiple climatic factors were often neglected, which contribute to the confusion of the dominant climatic factor driving IAV of net land carbon fluxes. Despite major advances in physiological understanding on ecosystem response to climatic variations, current studies disproportionately focus on tropical forests. Future studies should fill the gap over more arid tropical ecosystems, such as savannas, shrublands and grasslands.

The carbon cycle sensitivity to interannual climatic variations is proven to be an effective metric to evaluate model performance on IAV of photosynthesis, respiration and net land carbon flux (Piao et al., 2013; Huntzinger et al., 2017). In addition, changes in the magnitude of variability might serve as a potential early warning signal for more abrupt change. However, we caution that the challenges to applying metrics derived from IAV to predict carbon-climate feedbacks are greater than what was shown in previous emergent constrain studies. Capturing interannual variability does not necessarily lead to better prediction of carbon-climate feedbacks in future due to missing critical slow-evolving processes, but it helps improving our confidence that, at least, fundamental processes at interannual time-scale for current climate are robustly represented in the carbon cycle models. Advancing our understanding to IAV of the carbon cycle requires new technologies to measure globally the component fluxes of the net land carbon flux to better disentangle process contributions and improved ESMs to properly integrate process knowledge learnt at spatial scales from sites to the globe.

Acknowledgements

This study was supported by the National Natural Science Foundation of China (41530528) and the 111 Project (B14001). We thank Dr. Corinne Le Quéré for helpful discussions in preparing the manuscript. We thank TRENDY modelling group and CMIP5 community for providing DGVM and ESM simulation data. The authors declare no conflicts of interest.

Table 1. Summary of studies on the relationship between interannual variations (IAV) of global net land carbon flux and climatic variables

Proxy for IAV of global net land flux[1]	**Proxy for temperature IAV**	**Proxy for IAV of water availability**[2]	**Considered interactions between temperature and water availability**[3]	**R_T**[4]	**R_P**[5]	**S_T (PgC yr^{-1} $^{o}C^{-1}$)**[6]	**S_P (PgC yr^{-1} 100 mm^{-1})**[7]	**Time period**	**Climate aggregation**[8]	**Reference**
CGR	mean	precipitation	no	0.65	-0.3	-	-	1960-2003	30N - 30S	Adams et al., 2005
CGR	mean	precipitation	no	0.55	-0.25	-	-	1960-2003	global	Adams et al., 2005
CGR	mean	-	no	0.65	-	5.1	-	1960-2009	30N - 30S (L&O)	Cox et al., 2013
CGR	mean	precipitation	no	0.7	-0.5	3.5	-	1959-2011	24N - 24S	Wang et al., 2013
CGR	mean	precipitation	case 1	0.53	-0.19	2.7 - 5.5	-	1959-2009	23N - 23S	Wang et al., 2014

CGR	mean	precipitation, PDSI	no	0.68	-0.58 (precipitation) -0.65 (PDSI)	2.4	-1.1	1997-2011	global	Keppel-Aleks et al., 2014
RLS	nighttime	precipitation	no	0.56	-0.19	-	-	1959-2010	30N - 30S	Anderegg et al., 2015
NEE	mean	precipitation	no	0.94	-0.37	-	-	1980-2013	global	Jung et al., 2017
CGR	mean	precipitation	no	0.77	0.63	2.92	-0.46	1960-2012	23N - 23S	Wang et al., 2016
CGR	mean	precipitation	case 2	0.54	0.03	2.6	-0.1	1959-2010	30N - 30S	Fang et al., 2017
CGR	mean	TWS	no	0.18 - 0.57	-0.65 - -0.85	3.89	-	1980-2016[9]	global	Humphrey et al., 2018
CGR	mean	TWS	no	0.53 - 0.77	-0.65 - -0.75	-	-	1980-2016[9]	24N - 24S	Humphrey et al., 2018
NLS	mean	-	no	-	-	2.8 - 4.1	-	1957-2016	25N - 25S	Rodenbeck et al., 2018

CGR	mean	-	no	-	-	5.9	-	1960-2017	30N - 30S (L&O)	Chylek et al., 18

[1] proxy for IAV global net land carbon flux includes: atmospheric CO_2 growth rate (CGR), residual land sink (RLS) as the residual mass balance of other term (fossil fuel emission, CGR, ocean sink and land use change emission) of the global carbon budget (see Le Quere et al., 2018), net ecosystem exchange (NEE) as the empirical scale-up of eddy-covariance measurements (see Tramontana et al., 2016); net land sink (NLS) derived from atmospheric inversions, which includes both net ecosystem exchange and land use change emission (see Rodenbeck et al., 2018).

[2] proxy for IAV of water availability includes: annual precipitation, Palmer Drought Severity Index (PDSI), terrestrial water storage (TWS)

[3] Consideration of interactions between temperature and water availability index: in case 1, temperature sensitivity of CGR is regulated by water availability; in case 2, temperature/precipitation sensitivity of CGR is different between El Nino and La Nina years.

[4] correlation/partial correlation between IAV of net land carbon flux and temperature. The lead/lag of time series is applied in some studies.

[5] correlation/partial correlation between IAV of net land carbon flux and water availability. When more than one proxy of water availability are used, the bracket after the number indicates the water availability index used. The lead/lag of time series is applied in some studies.

[6] Sensitivity of IAV of net land carbon flux to temperature IAV, often termed as γ^{IAV} in the literature. When γ^{IAV} of different periods were reported, we presented the range here.

[7] Sensitivity of IAV of net land carbon flux to precipitation IAV

[8] aggregation of climate variable over spatial domain. Most studies only consider land area. When land and ocean area were both considered, it is noted as (L&O).

[9] In this study, the time-length of correlation between CGR and temperature and the correlation between CGR and TWS are not the same due to different time coverage of temperature and TWS data. Data were extracted from its Figure 2.

Figure legends

Figure 1. Comparison of interannual variations (IAV) of atmospheric CO_2 growth rate extracted by six methods. (a) magnitude of variance (standard deviations) of IAV and longer-term trend of CO_2 growth rate. (b) Matrix of correlation between IAV extracted from different methods. Correlation coefficients in the upper-left triangle and statistical significance (P-value) in the lower-right triangle. The six IAV extraction methods are: Fast Fourier Transformation (FFT), Ensemble Empirical Mode Decomposition (EEMD) and Singular Spectrum Analysis (SSA), and three smoothing-filter methods (no smoothing (SMN), smoothing with a short (6 month) time window (SMS), and smoothing with a long (13 month) time window (SML)). For frequency component decomposition methods (FFT, EEMD and SSA), the monthly CO_2 growth rate was decomposed into seasonal (<16 months), IAV (16 months – 128 months) and long-term trend signals (>128 month). For three other methods, seasonal variability was removed by taking the difference between the CO_2 concentration in one month and the same month in the previous year, and applying the smoothing filter of different window length. The linear trend was extracted with the least-square fitting.

Figure 2. Interannual variations (IAV) in detrended anomalies of the global CO_2 budget components (left) and their standard deviation of IAV (right) for the period 1980-2017. The global CO_2 budget components include CO_2 growth rate (CGR, black), fossil fuel emissions (light grey), land use change emission (purple), net land carbon flux estimated by land carbon cycle models (LM, light green) and by atmospheric inversion models (INV, dark green), ocean net carbon flux estimated by ocean carbon cycle models (OM, light blue) and atmospheric inversion models (INV, dark blue), and fire emission derived from Global Fire Emission Dataset (GFEDv4.1s, yellow). Positive values indicate anomalies that tend to increase CGR anomalies (e.g. releasing more carbon to or uptake less carbon from the atmosphere). Error bars indicate inter-model standard deviation of the detrended anomaly each year (left panel) and that of the s.d. for interannual variation of each CO_2 budget component (right panel). Note that GFEDv4.1s fire emission is only

available since 1997. See Table S1 for details of datasets used.

Figure 3. Spatial distribution of interannual variations (IAV) of net land carbon flux. (a) Spatial distribution of the standard deviation (s.d.) for IAV in detrended anomalies of net land carbon flux. The s.d. for IAV is estimated by the average of sixteen land carbon cycle model (LM), the average of two atmospheric inversion models (INV) and the average of 36 FLUXCOM models derived from three machine learning methods, shown as an RGB image map. Redder the grid cell is, larger the s.d. at this grid cell estimated by LM is, relatively to the maximum of IAV s.d. estimated by LM. Similarly, greener grid cell means larger s.d. of IAV estimated by INV and bluer grid cell means larger s.d. of IAV estimated by FLUXCOM. Brighter pixels indicate larger IAV than the darker pixels. (b) Regional contribution to global net carbon flux IAV. Global land is divided into four different regions: tropical non-semi-arid ecosystems, tropical semi-arid ecosystems, extra-tropical semi-arid ecosystems and others. The definition of semi-arid region and calculation of regional contributions follow Ahlström et al. (2015) (c) Contribution of each grid cell to global net land carbon flux IAV projected in the climate space. T indicates mean annual temperature of this grid while P-PET indicates the water deficit between mean annual precipitation (P) and potential evapotranspiration (PET).

Figure 4. Explained interannual variation (R^2) of gross primary productivity (GPP) and terrestrial ecosystem respiration (TER) on net carbon flux (a) and spatial distribution of the difference estimated by the average of sixteen land carbon cycle models (LM) (b), FLUXCOM (c) and FLUXNET (d). In panel b-d, a blue color indicates that IAV in net carbon flux are more driven by IAV in GPP than by TER. A red color indicates the opposite. Black dots in panel b and c indicate grids where more than 75% of the models (12 of 16 LM or 27 of 36 FLUXCOM models) agree on the sign of the difference. Inset in panel d shows histogram of the R^2 difference in FLUXNET sites. IAV in carbon fluxes are obtained as detrended annual value. In panel a, GPP and TER are ensemble mean of 16 LMs. Only FLUXNET sites with more than 5-years of data are shown in panel d.

Figure 5. Anomalies of net carbon flux in El Niño, La Niña and Volcanic eruption years. The anomalies in El Niño year were the average of net carbon flux anomalies in three strongest El Niño years (1987, 1997 and 2015) and those in La Niña year were the average of net carbon flux anomalies in three strongest La Niña years (1989, 1999 and 2011). The anomalies in volcanic eruption years were the average of net carbon flux anomalies in years after the strongest volcanic eruption (El Chichón (1982-1983) and Pinatubo (1991-1992)). Grey area in the patterns of land carbon cycle models (LM) and FLUXCOM indicate grids where less than 75% of the models (12 of 16 LM or 27 of 36 FLUXCOM models) agree on the sign of the anomalies.

Figure 6. Partial correlation between interannual variations (IAV) in net carbon fluxes and those in annual temperature and precipitation. (a) Partial correlation coefficients between tropical net land carbon flux anomaly and tropical annual temperature/precipitation anomaly. Symbols show detrended anomalies of tropical net land carbon flux were estimated by atmospheric CO_2 growth rate (CGR), land carbon cycle models (LM), atmospheric inversion models (INV) and FLUXCOM models. Spatial pattern of partial correlation between local temperature or precipitation anomaly and local net land carbon flux anomaly estimated by LM, INV, FLUXCOM and FLUXNET are shown in panel b, c, d, respectively. The latitudinal distribution of partial correlation coefficients between latitudinal average of net land carbon flux and temperature (T) or precipitation (P) is shown on the right of panel b-d. Note 1991-1993 are excluded from the correlation analyses because variations in the post-Pinatubo are known to be affected by factors other than climatic variations.

Figure 7. The structure equation model on the relationship of the direct and indirect effects on IAV of CO_2 growth rate during 1980-2016. Blue arrows indicate negative relationships while red arrows indicate positive relationships. Single-headed solid arrows indicate significant relationship ($P < 0.05$) with the arrow thickness proportional to the strength of the relationship (standardized coefficient shown besides the arrow). Double-headed grey arrows indicate covariations between

variables. R^2 on the top right indicates the variance of CGR explained by the SEM. RMSEA is the Root Mean Square Error of Approximation. AGFI is the Adjusted Goodness-of-Fit Index provide an absolute metric for how well the model describes the data. It ranges between 0 (bad) and 1 (perfect).

Figure 8. Regional contributions to net land carbon flux, GPP and TER anomalies at seasonal, interannual, decadal and centennial timescales. Carbon fluxes were estimated by eighteen CMIP5 climate-carbon-cycle models for the period 1861-2099 (Table S1). Variations at seasonal, interannual, decadal and centennial time scales were extracted with Fast Fourier Transformation. The left four panels show the spatial pattern of contributions of Net biome productivity (NBP) anomalies in grid cells to global NBP anomalies at different timescales. Contributions of carbon flux (NBP, gross primary productivity GPP or total ecosystem respiration TER) anomalies in latitudinal bands to global carbon flux anomalies at the corresponding timescales are shown in the right panels. Error bars indicate inter-model standard deviation.

Figure 9. Contribution of land and ocean carbon flux to its sum at seasonal, interannual, decadal and centennial timescales. Carbon fluxes were estimated by fourteen CMIP5 climate-carbon-cycle models for the period 1861-2099 with both land and ocean flux available (Table S1). Similar with Figure 8, variations at seasonal, interannual, decadal and centennial timescales were extracted with Fast Fourier Transformation. Error bars indicate inter-model standard deviation.

References

Adams, J. M., & Piovesan, G. (2005). Long series relationships between global interannual CO_2 increment and climate: Evidence for stability and change in role of the tropical and boreal-temperate zones. *Chemosphere, 59*, 1595-1612. doi:10.1016/j.chemosphere.2005.03.064

Ahlström, A., Raupach, M. R., Schurgers, G., Smith, B., Arneth, A., Jung, M., . . . Zeng, N. (2015). The dominant role of semi-arid ecosystems in the trend and variability of the land CO_2 sink. *Science, 348*, 895-899.

Anderegg, W. R. L., Ballantyne, A. P., Smith, W. K., Majkut, J., Rabin, S., Beaulieu, C., . . . Pacala, S. W. (2015). Tropical nighttime warming as a dominant driver of variability in the terrestrial carbon sink. *Proceedings of the National Academy of Sciences, 112*, 15591-15596.

Anderson, L. O., Neto, G. R., Cunha, A. P., Fonseca, M. G., Moura, Y. M. d., Dalagnol, R., . . . de Aragão, L. E. O. e. C. (2018). Vulnerability of Amazonian forests to repeated droughts. *Philosophical Transactions of the Royal Society B: Biological Sciences, 373*, 20170411. doi:doi:10.1098/rstb.2017.0411

Angert, A., Biraud, S., Bonfils, C., Buermann, W., & Fung, I. (2004). CO_2 seasonality indicates origins of post-Pinatubo sink. *Geophysical Research Letters, 31*, L11103. doi:10.1029/2004gl019760

Aragão, L. E. O. C., Malhi, Y., Barbier, N., Lima, A., Shimabukuro, Y., Anderson, L., & Saatchi, S. (2008). Interactions between rainfall, deforestation and fires during recent years in the Brazilian Amazonia. *Philosophical Transactions of the Royal Society B: Biological Sciences, 363*, 1779-1785. doi:10.1098/rstb.2007.0026

Aragão, L. E. O. C., Anderson, L. O., Fonseca, M. G., Rosan, T. M., Vedovato, L. B., Wagner, F. H., . . . Saatchi, S. (2018). 21st Century drought-related fires counteract the decline of Amazon deforestation carbon emissions. *Nature Communications, 9*, 536. doi:10.1038/s41467-017-02771-y

Arneth, A., Harrison, S. P., Zaehle, S., Tsigaridis, K., Menon, S., Bartlein, P. J., . . . Vesala, T. (2010). Terrestrial biogeochemical feedbacks in the climate system. *Nature Geoscience, 3*, 525-532.

Arneth, A., Sitch, S., Pongratz, J., Stocker, B., Ciais, P., Poulter, B., . . . Chini, L. (2017). Historical carbon dioxide emissions caused by land-use changes are possibly larger than assumed. *Nature Geoscience, 10*, 79.

Arora, V. K., Boer, G. J., Friedlingstein, P., Eby, M., Jones, C. D., Christian, J. R., . . . Wu, T. (2013). Carbon–Concentration and Carbon–Climate Feedbacks in CMIP5 Earth System Models. *Journal of Climate, 26*, 5289-5314. doi:10.1175/JCLI-D-12-00494.1

Aubinet, M., Hurdebise, Q., Chopin, H., Debacq, A., De Ligne, A., Heinesch, B., . . . Vincke, C. (2018). Inter-annual variability of Net Ecosystem Productivity for a temperate mixed forest: A predominance of carry-over effects? *Agricultural And Forest Meteorology, 262*, 340-353.

Aubry-Kientz, M., Rossi, V., Wagner, F., & Hérault, B. (2015). Identifying climatic drivers of tropical forest dynamics. *Biogeosciences, 12*, 5583-5596. doi:10.5194/bg-12-5583-2015

Bacastow, R. B. (1976). Modulation of atmospheric carbon dioxide by the Southern Oscillation. *Nature, 261*, 116-118. doi:10.1038/261116a0

Baker, D. F., Law, R. M., Gurney, K. R., Rayner, P., Peylin, P., Denning, A. S., . . . Zhu, Z. (2006). TransCom 3 inversion intercomparison: Impact of transport model errors on the interannual variability of regional CO_2 fluxes, 1988-2003. *Global Biogeochemical Cycles, 20*, GB1002. doi:10.1029/2004gb002439

Baldocchi, D., Ryu, Y., & Keenan, T. (2016). Terrestrial Carbon Cycle Variability. *F1000Research, 5*, F1000 Faculty Rev-2371. doi:10.12688/f1000research.8962.1

Baldocchi, D., Chu, H., & Reichstein, M. (2018). Inter-annual variability of net and gross ecosystem carbon fluxes: A review. *Agricultural and Forest Meteorology, 249*, 520-533.

Ballantyne, A. P., Alden, C. B., Miller, J. B., Tans, P. P., & White, J. W. C. (2012). Increase in observed net carbon dioxide uptake by land and oceans during the past 50 years. *Nature, 488*, 70-72.

Bond-Lamberty, B., Bailey, V. L., Chen, M., Gough, C. M., & Vargas, R. (2018). Globally rising soil heterotrophic respiration over recent decades. *Nature, 560*, 80-83.

Bousquet, P., Peylin, P., Ciais, P., C, L. Q., Friedlingstein, P., & Tans, P. (2000). Regional changes in carbon dioxide fluxes of land and oceans since 1980. *Science, 290*, 1342.

Brando, P. M., Balch, J. K., Nepstad, D. C., Morton, D. C., Putz, F. E., Coe, M. T., . . . Nóbrega, C. C. (2014). Abrupt increases in Amazonian tree mortality due to drought–fire interactions. *Proceedings of the National Academy of Sciences*, 111, 6347-6352.

Braswell, B. H., Schimel, D. S., Linder, E., & Moore, B., III. (1997). The Response of Global Terrestrial Ecosystems to Interannual Temperature Variability. *Science, 278*, 870-873. doi:10.1126/science.278.5339.870

Brienen, R. J. W., Phillips, O. L., Feldpausch, T. R., Gloor, E., Baker, T. R., Lloyd, J., . . . Zagt, R. J. (2015). Long-term decline of the Amazon carbon sink. *Nature, 519*(7543), 344-348.

Brovkin, V., Loren, S., Jungclaus, J., Raddatz, T., Timmreck, C., Reick, C., . . . Six, K. (2010). Sensitivity of a coupled climate-carbon cycle model to large volcanic eruptions during the last millennium. *Tellus B: Chemical and Physical Meteorology, 62*, 674-681.

Burba G., 2019. *Illustrative Maps of Past and Present Eddy Covariance Measurement Locations: II. High-Resolution Images*. Retrieved August 6, 2019, from https://www.researchgate.net. 9 pp. DOI: 10.13140/RG.2.2.33191.70561

Caldwell, P. M., Bretherton, C. S., Zelinka, M. D., Klein, S. A., Santer, B. D., & Sanderson, B. M. (2014). Statistical significance of climate sensitivity predictors obtained by data mining. *Geophysical Research Letters, 41*, 1803-1808.

Chen, X., Zhang, X., Church, J. A., Watson, C. S., King, M. A., Monselesan, D., . . . Harig, C. (2017). The increasing rate of global mean sea-level rise during 1993–2014. *Nature Climate Change, 7*, 492.

Chevallier, F., Ciais, P., Conway, T. J., Aalto, T., Anderson, B. E., Bousquet, P., . . . Worthy, D. (2010). CO_2 surface fluxes at grid point scale estimated from a global 21 year reanalysis of atmospheric measurements. *Journal Of Geophysical Research, 115*, D21307. doi:10.1029/2010jd013887

Chylek, P., Tans, P., Christy, J., & Dubey, M. K. (2018). The carbon cycle response to two El Niño types: an observational study. *Environmental Research Letters, 13*, 024001.

Ciais, P., Dolman, A. J., Bombelli, A., Duren, R., Peregon, A., Rayner, P. J., ... Zehner, C. (2013).

Current systematic carbon-cycle observations and the need for implementing a policy-relevant carbon observing system. *Biogeosciences*, *11*, 3547-3602.

Ciais, P., Reichstein, M., Viovy, N., Granier, A., Ogee, J., Allard, V., . . . Valentini, R. (2005). Europe-wide reduction in primary productivity caused by the heat and drought in 2003. *Nature, 437*, 529-533.

Ciais, P., Piao, S. L., Cadule, P., Friedlingstein, P., & Chédin, A. (2009). Variability and recent trends in the African terrestrial carbon balance. *Biogeosciences, 6*, 1935-1948.

Clark, D. A., Piper, S. C., Keeling, C. D., & Clark, D. B. (2003). Tropical rain forest tree growth and atmospheric carbon dynamics linked to interannual temperature variation during 1984–2000. *Proceedings of the National Academy of Sciences, 100*, 5852-5857.

Clark, D. A., Clark, D. B., & Oberbauer, S. F. (2013). Field-quantified responses of tropical rainforest aboveground productivity to increasing CO_2 and climatic stress, 1997–2009. *Journal of Geophysical Research: Biogeosciences, 118*, 783-794.

Corlett, R. T. (2011). Impacts of warming on tropical lowland rainforests. *Trends in Ecology and Evolution, 26*, 606-613.

Corlett, R. T. (2016). The Impacts of Droughts in Tropical Forests. *Trends In Plant Science, 21*, 584-593.

Cox, P., & Jones, C. (2008). Illuminating the Modern Dance of Climate and CO_2. *Science, 321*, 1642-1644. doi:10.1126/science.1158907

Cox, P. M., Pearson, D., Booth, B. B., Friedlingstein, P., Huntingford, C., Jones, C. D., & Luke, C. M. (2013). Sensitivity of tropical carbon to climate change constrained by carbon dioxide variability. *Nature, 494*, 341-344.

Crowell, S. M. R., Randolph Kawa, S., Browell, E. V., Hammerling, D. M., Moore, B., Schaefer, K., & Doney, S. C. (2018). On the Ability of Space-Based Passive and Active Remote Sensing Observations of CO_2 to Detect Flux Perturbations to the Carbon Cycle. *Journal of Geophysical Research: Atmospheres, 123*, 1460-1477. doi:10.1002/2017jd027836

Crowther, T. W., Todd-Brown, K. E. O., Rowe, C. W., Wieder, W. R., Carey, J. C., Machmuller, M. B., . . . Bradford, M. A. (2016). Quantifying global soil carbon losses in response to warming. *Nature, 540*, 104. doi:10.1038/nature20150

da Costa, A. C. L., Galbraith, D., Almeida, S., Portela, B. T. T., Da Costa, M., De Athaydes Silva Junior, J., . . . Meir, P. (2010). Effect of 7 yr of experimental drought on vegetation dynamics and biomass storage of an eastern Amazonian rainforest. *New Phytologist, 187*, 579-591.

Doughty, C. E., & Goulden, M. L. (2008). Are tropical forests near a high temperature threshold? *Journal of Geophysical Research, 113*, G00B07. doi:10.1029/2007jg000632

Doughty, C. E., Metcalfe, D., Girardin, C., Amézquita, F. F., Cabrera, D. G., Huasco, W. H., . . . Rocha, W. (2015). Drought impact on forest carbon dynamics and fluxes in Amazonia. *Nature, 519*, 78.

Eldering, A., Wennberg, P. O., Crisp, D., Schimel, D., Gunson, M. R., Chatterjee, A., ... Weir, B. (2017). The Orbiting Carbon Observatory-2 early science investigations of regional carbon dioxide fluxes. *Science*, 358, eaam5745.

Fan, L., Wigneron, J.-P., Ciais, P., Chave, J., Brandt, M., Fensholt, R., . . . Peñuelas, J. (2019). Satellite-observed pantropical carbon dynamics. *Nature Plants*. doi:10.1038/s41477-019-0478-9

Fang, Y., Michalak, A. M., Schwalm, C. R., Huntzinger, D. N., Berry, J. A., Ciais, P., . . . Yang, J. (2017). Global land carbon sink response to temperature and precipitation varies with ENSO phase. *Environmental Research Letters, 12*, 064007.

FAO (Food and Agriculture Organization of the United Nations). (2010). Global Forest Resources Assessment 2010. *FAO forestry paper*, *163*.

Francey, R. J., Tans, P. P., Allison, C. E., Enting, I. G., White, J. W. C., & Trolier, M. (1995). Changes in oceanic and terrestrial carbon uptake since 1982. *Nature, 373*, 326-330.

Friedlingstein, P., Cox, P., Betts, R., Bopp, L., Von Bloh, W., Brovkin, V., . . . Zeng, N. (2006). Climate-carbon cycle feedback analysis: Results from the (CMIP)-M-4 model intercomparison. *Journal of Climate, 19*, 3337-3353.

Friend, A. D., Lucht, W., Rademacher, T. T., Keribin, R., Betts, R., Cadule, P., . . . Woodward, F. I. (2014). Carbon residence time dominates uncertainty in terrestrial vegetation responses to future climate and atmospheric CO_2. *Proceedings of the National Academy of Sciences, 111*, 3280-3285.

Froelich, N., Croft, H., Chen, J. M., Gonsamo, A., & Staebler, R. M. (2015). Trends of carbon fluxes and climate over a mixed temperate–boreal transition forest in southern Ontario, Canada. *Agricultural And Forest Meteorology, 211*, 72-84.

Gatti, L. V., Gloor, M., Miller, J. B., Doughty, C. E., Malhi, Y., Domingues, L. G., . . . Lloyd, J. (2014). Drought sensitivity of Amazonian carbon balance revealed by atmospheric measurements. *Nature, 506*, 76-80.

Gaubert, B., Stephens, B. B., Basu, S., Chevallier, F., Deng, F., Kort, E. A., ... & Schimel, D. (2019). Global atmospheric CO_2 inverse models converging on neutral tropical land exchange, but disagreeing on fossil fuel and atmospheric growth rate. *Biogeosciences*, *16*, 117-134.

Gloor, E., Wilson, C., Chipperfield Martyn, P., Chevallier, F., Buermann, W., Boesch, H., . . . Sullivan Martin, J. P. (2018). Tropical land carbon cycle responses to 2015/16 El Niño as recorded by atmospheric greenhouse gas and remote sensing data. *Philosophical Transactions of the Royal Society B: Biological Sciences, 373*, 20170302.

Grace, J. B. (2006). *Structural equation modeling and natural systems*: Cambridge University Press.

Gu, L., Baldocchi, D. D., Wofsy, S. C., Munger, J. W., Michalsky, J. J., Urbanski, S. P., & Boden, T. A. (2003). Response of a Deciduous Forest to the Mount Pinatubo Eruption: Enhanced Photosynthesis. *Science, 299*, 2035-2038. doi:10.1126/science.1078366

Gu, G., & Adler, R. F. (2011). Precipitation and Temperature Variations on the Interannual Time Scale: Assessing the Impact of ENSO and Volcanic Eruptions. *Journal of Climate, 24*, 2258-2270.

Gurney, K. R., Baker, D., Rayner, P., & Denning, S. (2008). Interannual variations in continental-scale net carbon exchange and sensitivity to observing networks estimated from atmospheric CO_2 inversions for the period 1980 to 2005. *Global Biogeochemical Cycles, 22*, GB3025. doi:10.1029/2007gb003082

Hall, A., Cox, P., Huntingford, C., & Klein, S. (2019). Progressing emergent constraints on future climate change. *Nature Climate Change, 9*, 269-278. doi:10.1038/s41558-019-0436-6

Hansis, E., Davis, S. J., & Pongratz, J. (2015). Relevance of methodological choices for accounting of land use change carbon fluxes. *Global Biogeochemical Cycles, 29*, 1230-1246. doi:doi:10.1002/2014GB004997

Hawinkel, P., Swinnen, E., Lhermitte, S., Verbist, B., Van Orshoven, J., & Muys, B. (2015). A time series processing tool to extract climate-driven interannual vegetation dynamics using Ensemble Empirical Mode Decomposition (EEMD). *Remote Sensing of Environment, 169*, 375-389. doi:https://doi.org/10.1016/j.rse.2015.08.024

Houghton, R. A. (2000). Interannual variability in the global carbon cycle. *Journal of Geophysical Research, 105*, 20121-20130. doi:10.1029/2000jd900041

Houghton, R. A. (2010). How well do we know the flux of CO_2 from land-use change? *Tellus B, 62*, 337-351. doi:10.1111/j.1600-0889.2010.00473.x

Houghton, R. A., & Nassikas, A. A. (2017). Global and regional fluxes of carbon from land use and land cover change 1850–2015. *Global Biogeochemical Cycles, 31*, 456-472. doi:doi:10.1002/2016GB005546

Houweling, S., Baker, D., Basu, S., Boesch, H., Butz, A., Chevallier, F., . . . Zhuravlev, R. (2015). An intercomparison of inverse models for estimating sources and sinks of CO_2 using GOSAT measurements. *Journal of Geophysical Research: Atmospheres, 120*, 5253-5266.

Huang, M., Piao, S., Ciais, P., Peñuelas, J., Wang, X., Keenan, T. F., . . . Janssens, I.A. (2019). Air temperature optima of vegetation productivity across global biomes. *Nature Ecology & Evolution*, 3, 772.

Humphrey, V., Zscheischler, J., Ciais, P., Gudmundsson, L., Sitch, S., & Seneviratne, S. I. (2018). Sensitivity of atmospheric CO_2 growth rate to observed changes in terrestrial water storage. *Nature, 560*, 628-631.

Huntzinger, D. N., Michalak, A. M., Schwalm, C., Ciais, P., King, A. W., Fang, Y., . . . Zhao, F. (2017). Uncertainty in the response of terrestrial carbon sink to environmental drivers undermines carbon-climate feedback predictions. *Scientific Reports, 7*, 4765. doi:10.1038/s41598-017-03818-2

IPCC (2012) Summary for policymakers. In: *Managing the Risks of Extreme Events and Disasters to Advance Climate Change Adaptation. A Special Report of Working Groups I and II of the Intergovernmental Panel on Climate Change* (eds Field CB, Barros V, Stocker TF et al.), pp. 1–19. Cambridge University Press, Cambridge, UK and New York, NY.

IPCC (2013) Summary for policymakers. In: *Climate Change 2013: The Physical Science Basis. Contribution of Working Group I to the Fifth Assessment Report of the Intergovernmental Panel on Climate Change* (eds Stocker TF, Qin D, Plattner G-K, Tignor M, Allen SK, Boschung J, Nauels A, Xia Y, Bex V, Midgley PM), pp. 3–29. Cambridge University Press, Cambridge, UK and New York, NY, USA.

Jensen, R., Herbst, M., & Friborg, T. (2017). Direct and indirect controls of the interannual variability in atmospheric CO_2 exchange of three contrasting ecosystems in Denmark. *Agricultural and Forest Meteorology, 233*, 12-31.

Jones, C. D., Collins, M., Cox, P. M., & Spall, S. A. (2001). The Carbon Cycle Response to ENSO: A Coupled Climate–Carbon Cycle Model Study. *Journal of Climate, 14*, 4113-4129.

Jones, C. D., & Cox, P. M. (2005). On the significance of atmospheric CO_2 growth rate anomalies in 2002-2003. *Geophysical Research Letters, 32*, L14816. doi:10.1029/2005gl023027

Jung, M., Reichstein, M., Margolis, H. A., Cescatti, A., Richardson, A. D., Arain, M. A., . . . Williams, C. (2011). Global patterns of land-atmosphere fluxes of carbon dioxide, latent heat, and sensible heat derived from eddy covariance, satellite, and meteorological observations. *Journal of Geophysical Research, 116*, G00J07. doi:10.1029/2010jg001566

Jung, M., Reichstein, M., Schwalm, C. R., Huntingford, C., Sitch, S., Ahlström, A., . . . Zeng, N. (2017). Compensatory water effects link yearly global land CO_2 sink changes to temperature. *Nature, 541*, 516-520.

Jung, M., Schwalm, C., Migliavacca, M., Walther, S., Camps-Valls, G., Koirala, S., . . . Carvalhais, N. (2019). Scaling carbon fluxes from eddy covariance sites to globe: Synthesis and evaluation of the FLUXCOM approach. *Biogeosciences Discussions*.

Keeling, C. D., Bacastow, R. B., Bainbridge, A. E., Ekdahl, C. A., Guenther, P. R., Waterman, L. S., & Chin, J. F. S. (1976). Atmospheric carbon dioxide variations at Mauna Loa Observatory, Hawaii. *Tellus, 28*, 538-551. doi:10.1111/j.2153-3490.1976.tb00701.x

Keeling, C. D., Piper, S. C., Bacastow, R. B., Wahlen, M., Whorf, T. P., Heimann, M., & Meijer, H. A. (2005). Atmospheric CO_2 and $^{13}CO_2$ exchange with the terrestrial biosphere and oceans from 1978 to 2000: Observations and carbon cycle implications. In *A history of atmospheric CO_2 and its effects on plants, animals, and ecosystems* (pp. 83-113). Springer, New York, NY.

Keeling, C., & Revelle, R. (1985). Effects of El Niño/Southern Oscillation on the atmospheric content of carbon dioxide. *Meteoritics, 20*, 437-450.

Keeling, C. D., Whorf, T. P., Wahlen, M., & van der Plichtt, J. (1995). Interannual extremes in the rate of rise of atmospheric carbon dioxide since 1980. *Nature, 375*, 666-670.

Keenan, T. F., Baker, I., Barr, A., Ciais, P., Davis, K., Dietze, M., . . . Richardson, A. D. (2012). Terrestrial biosphere model performance for inter-annual variability of land-atmosphere CO2 exchange. *Global Change Biology, 18*(6), 1971-1987.

Keenan, T. F., & Williams, C. A. (2018). The Terrestrial Carbon Sink. *Annual Review of Environment and Resources, 43*, 219-243. doi:10.1146/annurev-environ-102017-030204

Keppel-Aleks, G., Wolf, A. S., Mu, M., Doney, S. C., Morton, D. C., Kasibhatla, P. S., . . . Randerson, J. T. (2014). Separating the influence of temperature, drought, and fire on interannual variability in atmospheric CO_2. *Global Biogeochemical Cycles, 28*, 1295-1310.

Keppel-Aleks, G., Basile, S. J., & Hoffman, F. M. (2018). A Functional Response Metric for the Temperature Sensitivity of Tropical Ecosystems. *Earth Interactions, 22*, 1-20.

Kim, J.-S., Kug, J.-S., Yoon, J.-H., & Jeong, S.-J. (2016). Increased Atmospheric CO_2 Growth Rate during El Niño Driven by Reduced Terrestrial Productivity in the CMIP5 ESMs. *Journal of Climate, 29*, 8783-8805.

Kindermann, J., Würth, G., Kohlmaier, G. H., & Badeck, F. W. (1996). Interannual variation of carbon exchange fluxes in terrestrial ecosystems. *Global Biogeochemical Cycles, 10*, 737-755.

Knorr, W., Gobron, N., Scholze, M., Kaminski, T., Schnur, R., & Pinty, B. (2007). Impact of terrestrial biosphere carbon exchanges on the anomalous CO_2 increase in 2002-2003. *Geophysical Research Letters, 34*, L09703. doi:10.1029/2006gl029019

Koven, C. D., Lawrence, D. M., & Riley, W. J. (2015). Permafrost carbon−climate feedback is sensitive to deep soil carbon decomposability but not deep soil nitrogen dynamics. *Proceedings of the National Academy of Sciences, 112*, 3752-3757.

Kuze, A., Suto, H., Nakajima, M., & Hamazaki, T. (2009). Thermal and near infrared sensor for carbon observation Fourier-transform spectrometer on the Greenhouse Gases Observing Satellite for greenhouse gases monitoring. *Applied Optics*, 48, 6716-6733.

Langenfelds, R. L., Francey, R. J., Pak, B. C., Steele, L. P., Lloyd, J., Trudinger, C. M., & Allison, C. E. (2002). Interannual growth rate variations of atmospheric CO_2 and its $\delta^{13}C$, H_2, CH_4, and CO between 1992 and 1999 linked to biomass burning. *Global Biogeochemical Cycles, 16*, 1048. doi:10.1029/2001gb001466

Le Quéré, C., Andrew, R. M., Friedlingstein, P., Sitch, S., Hauck, J., Pongratz, J., . . . Zheng, B. (2018). Global Carbon Budget 2018. *Earth System Science Data, 10*, 2141-2194. doi:10.5194/essd-10-2141-2018

Lewis, S. L., Edwards, D. P., & Galbraith, D. (2015). Increasing human dominance of tropical forests. *Science, 349*, 827-832.

Liptak, J., Keppel-Aleks, G., & Lindsay, K. (2017). Drivers of multi-century trends in the atmospheric CO_2 mean annual cycle in a prognostic ESM. *Biogeosciences, 14*, 1383-1401. doi:10.5194/bg-14-1383-2017

Liu, J., Bowman, K. W., Schimel, D. S., Parazoo, N. C., Jiang, Z., Lee, M., . . . Eldering, A. (2017). Contrasting carbon cycle responses of the tropical continents to the 2015-2016 El Niño. *Science, 358*. doi:10.1126/science.aam5690

Liu, Y., Piao, S., Gasser, T., Ciais, P., Yang, H., Wang, H., . . . Wang, T. (2019). Field-experiment constraints on the enhancement of the terrestrial carbon sink by CO2 fertilization. *Nature Geoscience, 12*(10), 809-814.

Liu, Z., Ballantyne, A. P., Poulter, B., Anderegg, W. R. L., Li, W., Bastos, A., & Ciais, P. (2018). Precipitation thresholds regulate net carbon exchange at the continental scale. *Nature Communications, 9*, 3596.

Lucht, W., Prentice, I. C., Myneni, R. B., Sitch, S., Friedlingstein, P., Cramer, W., . . . Smith, B.

(2002). Climatic Control of the High-Latitude Vegetation Greening Trend and Pinatubo Effect. *Science, 296*, 1687-1689.

Mahecha, M. D., Reichstein, M., Carvalhais, N., Lasslop, G., Lange, H., Seneviratne, S. I., . . . Richardson, A. D. (2010). Global Convergence in the Temperature Sensitivity of Respiration at Ecosystem Level. *Science, 329*, 838-840.

Manzoni, S., Vico, G., Palmroth, S., Porporato, A., & Katul, G. (2013). Optimization of stomatal conductance for maximum carbon gain under dynamic soil moisture. *Advances In Water Resources, 62*, 90-105.

Marcolla, B., Rödenbeck, C., & Cescatti, A. (2017). Patterns and controls of inter-annual variability in the terrestrial carbon budget. *Biogeosciences, 14*, 3815-3829.

Melillo, J. M., Frey, S. D., DeAngelis, K. M., Werner, W. J., Bernard, M. J., Bowles, F. P., . . . Grandy, A. S. (2017). Long-term pattern and magnitude of soil carbon feedback to the climate system in a warming world. *Science, 358*, 101-105.

Mercado, L. M., Bellouin, N., Sitch, S., Boucher, O., Huntingford, C., Wild, M., & Cox, P. M. (2009). Impact of changes in diffuse radiation on the global land carbon sink. *Nature, 458*, 1014-1017.

Moser, G., Schuldt, B., Hertel, D., Horna, V., Coners, H., Barus, H., & Leuschner, C. (2014). Replicated throughfall exclusion experiment in an Indonesian perhumid rainforest: wood production, litter fall and fine root growth under simulated drought. *Global Change Biology, 20*, 1481-1497.

Mystakidis, S., Davin, E. L., Gruber, N., & Seneviratne, S. I. (2016). Constraining future terrestrial carbon cycle projections using observation-based water and carbon flux estimates. *Global Change Biology, 22*, 2198-2215.

Nepstad, D. C., de Carvalho, C. R., Davidson, E. A., Jipp, P. H., Lefebvre, P. A., Negreiros, G. H., . . . Vieira, S. (1994). The role of deep roots in the hydrological and carbon cycles of Amazonian forests and pastures. *Nature, 372*, 666. doi:10.1038/372666a0

Nepstad, D. C., Moutinho, P., Dias-Filho, M. B., Davidson, E., Cardinot, G., Markewitz, D., . . . Schwalbe, K. (2002). The effects of partial throughfall exclusion on canopy processes, aboveground production, and biogeochemistry of an Amazon forest. *Journal of Geophysical Research, 107*, 8085. doi:10.1029/2001jd000360

Novick, K. A., Ficklin, D. L., Stoy, P. C., Williams, C. A., Bohrer, G., Oishi, A. C., . . . Phillips, R. P. (2016). The increasing importance of atmospheric demand for ecosystem water and carbon fluxes. *Nature Climate Change, 6*, 1023-1027.

O'Connell, C. S., Ruan, L., & Silver, W. L. (2018). Drought drives rapid shifts in tropical rainforest soil biogeochemistry and greenhouse gas emissions. *Nature Communications, 9*, 1348. doi:10.1038/s41467-018-03352-3

Oliveira, R. S., Dawson, T. E., Burgess, S. S. O., & Nepstad, D. C. (2005). Hydraulic redistribution in three Amazonian trees. *Oecologia, 145*, 354-363. doi:10.1007/s00442-005-0108-2

Palmer, P. I., Feng, L., Baker, D., Chevallier, F., Bösch, H., & Somkuti, P. (2019). Net carbon emissions from African biosphere dominate pan-tropical atmospheric CO_2 signal. *Nature Communications, 10*, 3344. doi:10.1038/s41467-019-11097-w

Pan, Y., Birdsey, R. A., Fang, J., Houghton, R., Kauppi, P. E., Kurz, W. A., . . . Hayes, D. (2011). A Large and Persistent Carbon Sink in the World's Forests. *Science, 333*, 988-993.

Patra, P. K., Maksyutov, S., Ishizawa, M., Nakazawa, T., Takahashi, T., & Ukita, J. (2005). Interannual and decadal changes in the sea-air CO_2 flux from atmospheric CO_2 inverse modeling. *Global Biogeochemical Cycles, 19*, GB4013. doi:10.1029/2004GB002257

Peñuelas, J., Ciais, P., Canadell, J. G., Janssens, I. A., Fernández-Martínez, M., Carnicer, J., . . . Sardans, J. (2017). Shifting from a fertilization-dominated to a warming-dominated period. *Nature Ecology & Evolution, 1*, 1438-1445. doi:10.1038/s41559-017-0274-8

Peylin, P., Law, R. M., Gurney, K. R., Chevallier, F., Jacobson, A. R., Maki, T., . . . Zhang, X. (2013). Global atmospheric carbon budget: results from an ensemble of atmospheric CO_2 inversions. *Biogeosciences, 10*, 6699-6720.

Phillips, O. L., Aragao, L. E. O. C., Lewis, S. L., Fisher, J. B., Lloyd, J., Lopez-Gonzalez, G., . . . Torres-Lezama, A. (2009). Drought sensitivity of the Amazon rainforest. *Science, 323*, 1344-1347.

Piao, S., Ciais, P., Friedlingstein, P., de Noblet-Ducoudré, N., Cadule, P., Viovy, N., & Wang, T. (2009). Spatiotemporal patterns of terrestrial carbon cycle during the 20th century. *Global Biogeochemical Cycles, 23*, GB4026. doi:10.1029/2008gb003339

Piao, S., Sitch, S., Ciais, P., Friedlingstein, P., Peylin, P., Wang, X., . . . Zeng, N. (2013). Evaluation of terrestrial carbon cycle models for their response to climate variability and to CO_2 trends. *Global Change Biology, 19*, 2117-2132.

Piao, S., Liu, Z., Wang, T., Peng, S., Ciais, P., Huang, M., . . . Tans, P. P. (2017). Weakening temperature control on the interannual variations of spring carbon uptake across northern lands. *Nature Climate Change, 7*, 359-363.

Pongratz, J., Reick, C. H., Houghton, R. A., & House, J. I. (2014). Terminology as a key uncertainty in net land use and land cover change carbon flux estimates. *Earth System Dynamics, 5*, 177-195.

Poulter, B., Frank, D., Ciais, P., Myneni, R. B., Andela, N., Bi, J., . . . van der Werf, G. R. (2014). Contribution of semi-arid ecosystems to interannual variability of the global carbon cycle. *Nature, 509*, 600-603.

Randerson, J. T., Lindsay, K., Munoz, E., Fu, W., Moore, J. K., Hoffman, F. M., . . . Doney, S. C. (2015). Multicentury changes in ocean and land contributions to the climate-carbon feedback. *Global Biogeochemical Cycles, 29*(6), 744-759.

Raupach, M. R., Canadell, J. G., & Le Quéré, C. (2008). Anthropogenic and biophysical contributions to increasing atmospheric CO_2 growth rate and airborne fraction. *Biogeosciences, 5*, 1601-1613. doi:10.5194/bg-5-1601-2008

Rayner, P. J., Law, R. M., Allison, C. E., Francey, R. J., Trudinger, C. M., & Pickett-Heaps, C. (2008). Interannual variability of the global carbon cycle (1992-2005) inferred by inversion of atmospheric CO_2 and $^{13}CO_2$ measurements. *Global Biogeochemical Cycles, 22*, GB3008. doi:10.1029/2007gb003068

Reich, P. B., Sendall, K. M., Stefanski, A., Rich, R. L., Hobbie, S. E., & Montgomery, R. A. (2018). Effects of climate warming on photosynthesis in boreal tree species depend on soil moisture. *Nature, 562*, 263. doi:10.1038/s41586-018-0582-4

Rödenbeck, C., Houweling, S., Gloor, M., & Heimann, M. (2003). CO_2 flux history 1982–2001 inferred from atmospheric data using a global inversion of atmospheric transport. *Atmospheric Chemistry and Physics, 3*, 1919-1964.

Rödenbeck, C., Zaehle, S., Keeling, R., & Heimann, M. (2018a). How does the terrestrial carbon exchange respond to inter-annual climatic variations? A quantification based on atmospheric CO_2 data. *Biogeosciences, 15*, 2481-2498.

Rödenbeck, C., Zaehle, S., Keeling, R., & Heimann, M. (2018b). History of El Niño impacts on the global carbon cycle 1957–2017: a quantification from atmospheric CO_2 data. *Philosophical Transactions of the Royal Society B: Biological Sciences, 373*, 20170303.

Roderick, M. L., Farquhar, G. D., Berry, S. L., & Noble, I. R. (2001). On the direct effect of clouds and atmospheric particles on the productivity and structure of vegetation. *Oecologia, 129*, 21-30.

Saatchi, S., Asefi-Najafabady, S., Malhi, Y., Aragão, L. E., Anderson, L. O., Myneni, R. B., & Nemani, R. (2013). Persistent effects of a severe drought on Amazonian forest canopy. *Proceedings of the National Academy of Sciences, 110*, 565-570.

Schneising, O., Reuter, M., Buchwitz, M., Heymann, J., Bovensmann, H., & Burrows, J. P. (2014). Terrestrial carbon sink observed from space: variation of growth rates and seasonal cycle amplitudes in response to interannual surface temperature variability. *Atmospheric Chemistry and Physics, 14*, 133-141. doi:10.5194/acp-14-133-2014

Schwalm, C. R., Williams, C. A., Schaefer, K., Arneth, A., Bonal, D., Buchmann, N., . . . Richardson, A. D. (2010). Assimilation exceeds respiration sensitivity to drought: A FLUXNET synthesis. *Global Change Biology, 16*, 657-670.

Shevliakova, E., Stouffer, R. J., Malyshev, S., Krasting, J. P., Hurtt, G. C., & Pacala, S. W. (2013). Historical warming reduced due to enhanced land carbon uptake. *Proceedings of the National Academy of Sciences, 110*, 16730-16735. doi:10.1073/pnas.1314047110

Shi, Z., Thomey, M., Mowll, W., Litvak, M., Brunsell, N. A., Collins, S., . . . Luo, Y. (2014). Differential effects of extreme drought on production and respiration: synthesis and modeling analysis. *Biogeosciences, 11*, 621-633.

Shiga, Y. P., Michalak, A. M., Fang, Y., Schaefer, K., Andrews, A. E., Huntzinger, D. H., . . . Wei, Y. (2018). Forests dominate the interannual variability of the North American carbon sink. *Environmental Research Letters, 13*, 084015.

Sillmann, J., Kharin, V. V., Zwiers, F. W., Zhang, X., & Bronaugh, D. (2013). Climate extremes indices in the CMIP5 multimodel ensemble: Part 2. Future climate projections. *Journal of Geophysical Research: Atmospheres*, *118*, 2473-2493.

Sitch, S., Friedlingstein, P., Gruber, N., Jones, S. D., Murray-Tortarolo, G., Ahlström, A., . . . Myneni, R. (2015). Recent trends and drivers of regional sources and sinks of carbon dioxide. *Biogeosciences, 12*, 653-679.

Smith, P. (2004). How long before a change in soil organic carbon can be detected? *Global Change Biology, 10*, 1878-1883.

Stocker, B. D., Zscheischler, J., Keenan, T. F., Prentice, I. C., Seneviratne, S. I., & Peñuelas, J. (2019). Drought impacts on terrestrial primary production underestimated by satellite monitoring. *Nature Geoscience*, *12*, 264.

Tans, P., & Keeling, R. (2014). Trends in atmospheric carbon dioxide. National Oceanic and Atmospheric Administration. Global Greenhouse Gas Reference Network. *http://www. esrl. noaa. gov/gmd/ccgg/trends/(Page consultée le 20 janvier 2014).*

Tan, Z.-H., Cao, M., Yu, G.-R., Tang, J.-W., Deng, X.-B., Song, Q.-H., . . . Zhang, Y.-P. (2013). High sensitivity of a tropical rainforest to water variability: Evidence from 10 years of inventory and eddy flux data. *Journal of Geophysical Research: Atmospheres, 118*, 9393-9400.

Tapley, B. D., Bettadpur, S., Ries, J. C., Thompson, P. F., & Watkins, M. M. (2004). GRACE measurements of mass variability in the Earth system. *Science*, *305*, 503-505.

Tramontana, G., Jung, M., Schwalm, C. R., Ichii, K., Camps-Valls, G., Ráduly, B., . . . Papale, D. (2016). Predicting carbon dioxide and energy fluxes across global FLUXNET sites with regression algorithms. *Biogeosciences, 13*, 4291-4313.

Urbanski, S., Barford, C., Wofsy, S., Kucharik, C., Pyle, E., Budney, J., . . . Munger, J. W. (2007). Factors controlling CO_2 exchange on timescales from hourly to decadal at Harvard Forest.

Journal of Geophysical Research: Biogeosciences, 112. doi:10.1029/2006jg000293

van der Laan-Luijkx, I. T., van der Velde, I. R., Krol, M. C., Gatti, L. V., Domingues, L. G., Correia, C. S. C., . . . Peters, W. (2015). Response of the Amazon carbon balance to the 2010 drought derived with CarbonTracker South America. *Global Biogeochemical Cycles, 29*, 1092-1108.

van der Werf, G. R., Randerson, J. T., Collatz, G. J., Giglio, L., Kasibhatla, P. S., Arellano, A. F., . . . Kasischke, E. S. (2004). Continental-scale partitioning of fire emissions during the 1997 to 2001 El Niño/La Niña period. *Science, 303*, 73-76.

van der Werf, G. R., Randerson, J. T., Giglio, L., Collatz, G. J., Mu, M., Kasibhatla, P. S., ... van Leeuwen, T. T. (2010). Global fire emissions and the contribution of deforestation, savanna, forest, agricultural, and peat fires (1997–2009). *Atmospheric chemistry and physics*, *10*, 11707-11735.

van der Werf, G. R., Randerson, J. T., Giglio, L., van Leeuwen, T. T., Chen, Y., Rogers, B. M., . . . Kasibhatla, P. S. (2017). Global fire emissions estimates during 1997–2016. *Earth System Science Data, 9*, 697-720. doi:10.5194/essd-9-697-2017

Wang, J., Zeng, N., Liu, Y., & Bao, Q. (2014a). To what extent can interannual CO_2 variability constrain carbon cycle sensitivity to climate change in CMIP5 Earth System Models? *Geophysical Research Letters, 41*, 3535-3544.

Wang, J., Zeng, N., & Wang, M. (2016). Interannual variability of the atmospheric CO_2 growth rate: roles of precipitation and temperature. *Biogeosciences, 13*, 2339-2352.

Wang, T., Liu, D., Piao, S., Wang, Y., Wang, X., Guo, H., . . . Zhao, Y. (2018a). Emerging negative impact of warming on summer carbon uptake in northern ecosystems. *Nature Communications, 9*, 5391. doi:10.1038/s41467-018-07813-7

Wang, W., Ciais, P., Nemani, R. R., Canadell, J. G., Piao, S., Sitch, S., . . . Myneni, R. B. (2013). Variations in atmospheric CO_2 growth rates coupled with tropical temperature. *Proceedings of the National Academy of Sciences, 110*, 13061-13066.

Wang, X., Liu, L., Piao, S., Janssens, I. A., Tang, J., Liu, W., . . . Xu, S. (2014b). Soil respiration under climate warming: differential response of heterotrophic and autotrophic respiration.

Global Change Biology, 20, 3229-3237.

Wang, X., Piao, S., Ciais, P., Friedlingstein, P., Myneni, R. B., Cox, P., . . . Chen, A. (2014c). A two-fold increase of carbon cycle sensitivity to tropical temperature variations. *Nature, 506*, 212-215.

Wang, X., Ciais, P., Wang, Y., & Zhu, D. (2018b). Divergent response of seasonally dry tropical vegetation to climatic variations in dry and wet seasons. *Global Change Biology, 24*, 4709-4717.

Wenzel, S., Cox, P. M., Eyring, V., & Friedlingstein, P. (2014). Emergent constraints on climate-carbon cycle feedbacks in the CMIP5 Earth system models. *Journal of Geophysical Research: Biogeosciences, 119*, 794-807.

Withey, K., Berenguer, E., Palmeira Alessandro, F., Espírito-Santo Fernando, D. B., Lennox Gareth, D., Silva Camila, V. J., . . . Barlow, J. (2018). Quantifying immediate carbon emissions from El Niño-mediated wildfires in humid tropical forests. *Philosophical Transactions of the Royal Society B: Biological Sciences, 373*, 20170312.

Wu, J., van der Linden, L., Lasslop, G., Carvalhais, N., Pilegaard, K., Beier, C., & Ibrom, A. (2012). Effects of climate variability and functional changes on the interannual variation of the carbon balance in a temperate deciduous forest. *Biogeosciences, 9*, 13-28.

Xu, L., Samanta, A., Costa, M. H., Ganguly, S., Nemani, R. R., & Myneni, R. B. (2011). Widespread decline in greenness of Amazonian vegetation due to the 2010 drought. *Geophysical Research Letters, 38*, L07402. doi:10.1029/2011gl046824

Yang, H., Piao, S., Huntingford, C., Peng, S., Ciais, P., Chen, A., . . . Zscheischler, J. (2019). Strong but Intermittent Spatial Covariations in Tropical Land Temperature. *Geophysical Research Letters, 46*, 356-364. doi:doi:10.1029/2018GL080463

Yang, Y., Saatchi, S. S., Xu, L., Yu, Y., Choi, S., Phillips, N., . . . Myneni, R. B. (2018). Post-drought decline of the Amazon carbon sink. *Nature Communications, 9*, 3172. doi:10.1038/s41467-018-05668-6

Yin, Y., Ciais, P., Chevallier, F., Li, W., Bastos, A., Piao, S., . . . Liu, H. (2018). Changes in the Response of the Northern Hemisphere Carbon Uptake to Temperature Over the Last Three

Decades. *Geophysical Research Letters, 45*, 4371-4380. doi:10.1029/2018gl077316

Yuan, W., Zheng, Y., Piao, S., Ciais, P., Lombardozzi, D., Wang, Y., . . . Yang, S. (2019). Increased atmospheric vapor pressure deficit reduces global vegetation growth. *Science Advances, 5*, eaax1396. doi:10.1126/sciadv.aax1396

Zaehle, S., & Dalmonech, D. (2011). Carbon–nitrogen interactions on land at global scales: current understanding in modelling climate biosphere feedbacks. *Current Opinion in Environmental Sustainability, 3*, 311-320.

Zeng, N., Mariotti, A., & Wetzel, P. (2005). Terrestrial mechanisms of interannual CO_2 variability. *Global Biogeochemical Cycles, 19*, GB1016. doi:10.1029/2004gb002273

Zhang, Q., Wang, Y. P., Pitman, A. J., & Dai, Y. J. (2011). Limitations of nitrogen and phosphorous on the terrestrial carbon uptake in the 20th century. *Geophysical Research Letters, 38*. doi:10.1029/2011GL049244

Zhang, X., Wang, Y. P., Peng, S., Rayner, P. J., Ciais, P., Silver, J. D., . . . Zheng, X. (2018). Dominant regions and drivers of the variability of the global land carbon sink across timescales. *Global Change Biology, 24*, 3954-3968.

Zhou, L., Zhou, X., Shao, J., Nie, Y., He, Y., Jiang, L., . . . Hosseini Bai, S. (2016). Interactive effects of global change factors on soil respiration and its components: a meta-analysis. *Global Change Biology, 22*, 3157-3169.

Zscheischler, J., Michalak, A. M., Schwalm, C., Mahecha, M. D., Huntzinger, D. N., Reichstein, M., . . . Zeng, N. (2014). Impact of large-scale climate extremes on biospheric carbon fluxes: An intercomparison based on MsTMIP data. *Global Biogeochemical Cycles, 28*, 585-600. doi:10.1002/2014GB004826

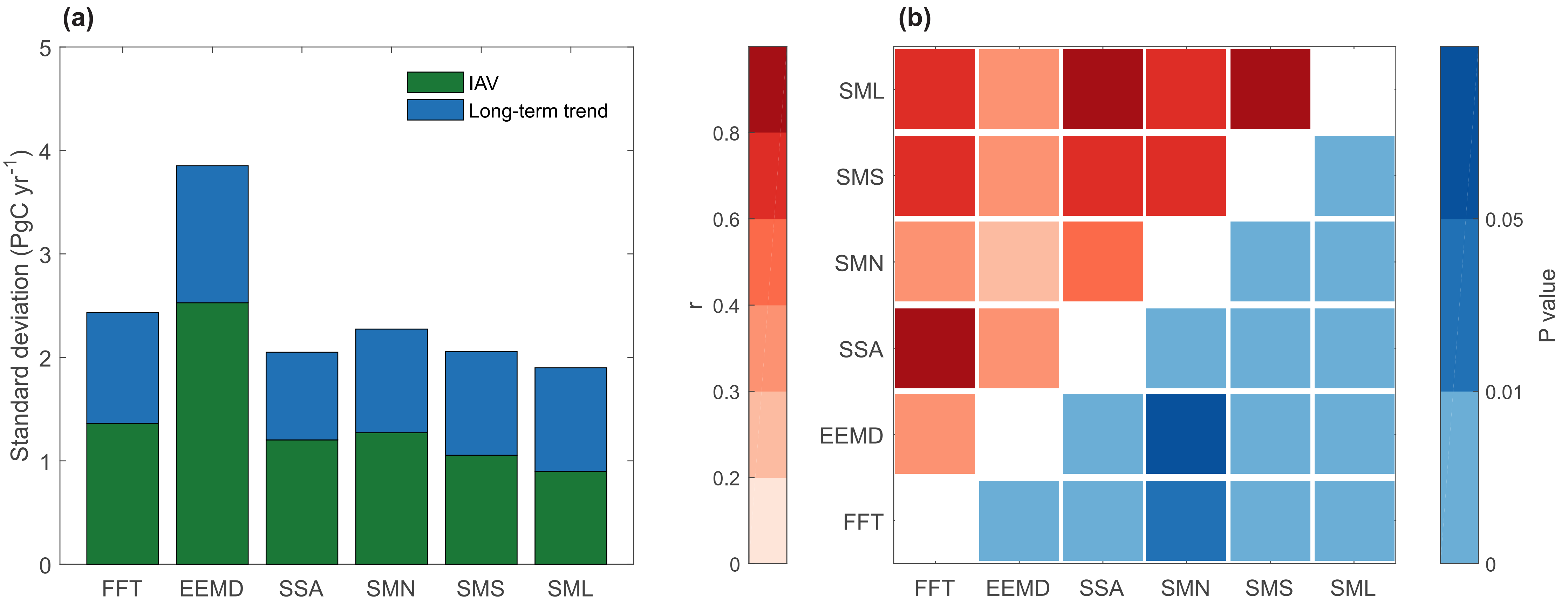

(a)
(b)
IAV
Long-term trend
Standard deviation (PgC yr-1)
FFT
EEMD
SSA
SMN
SMS
SML
r
P value
0
0.2
0.3
0.4
0.6
0.8
0.01
0.05

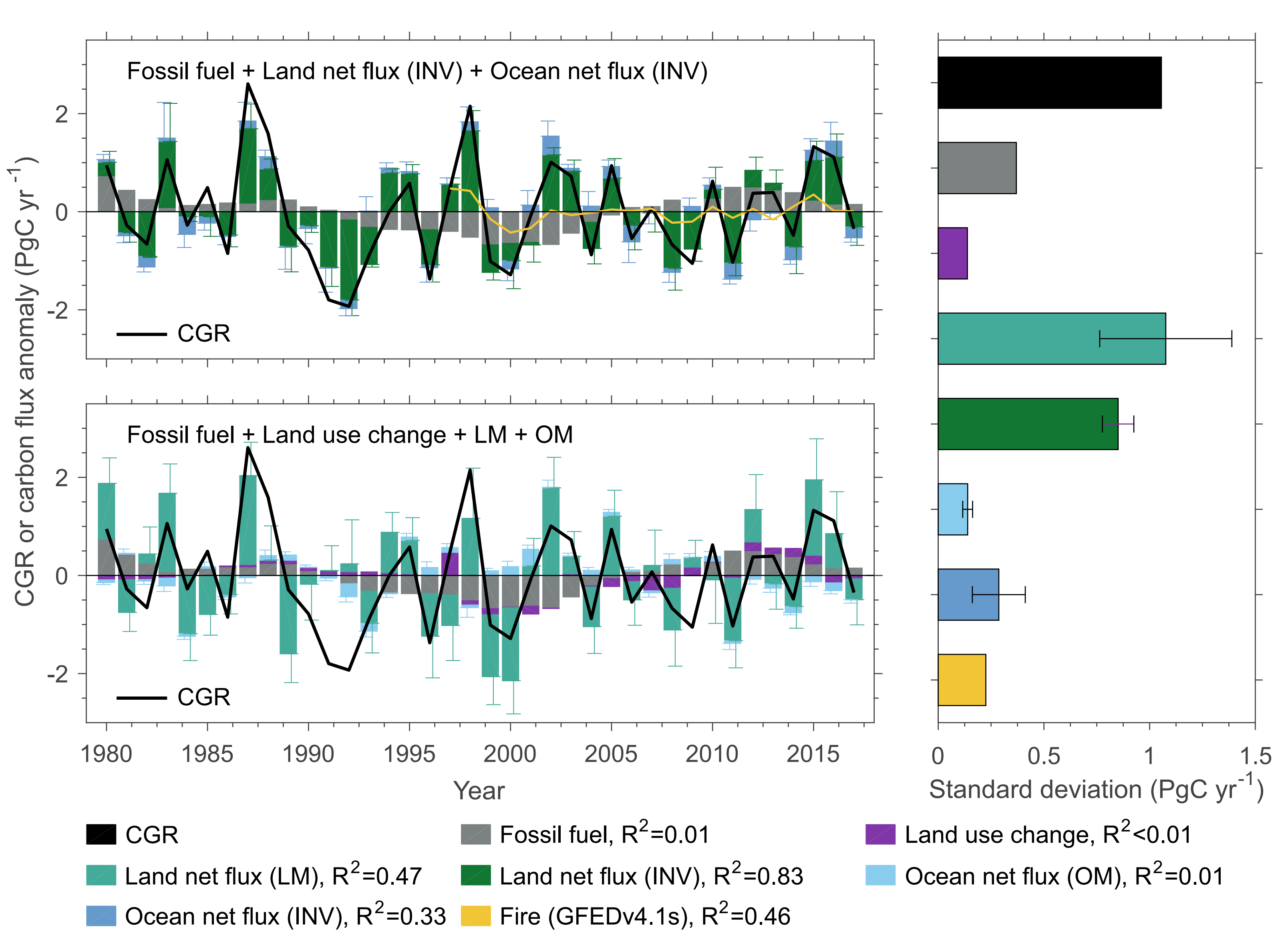

Fossil fuel + Land net flux (INV) + Ocean net flux (INV)
CGR
Fossil fuel + Land use change + LM + OM
CGR
CGR or carbon flux anomaly (PgC yr-1)
2
0
-2
1980
1985
1990
1995
2000
2005
2010
2015
Year
0
0.5
1
1.5
Standard deviation (PgC yr-1)
CGR
Fossil fuel, R2=0.01
Land use change, R2<0.01
Land net flux (LM), R2=0.47
Land net flux (INV), R2=0.83
Ocean net flux (OM), R2=0.01
Ocean net flux (INV), R2=0.33
Fire (GFEDv4.1s), R2=0.46

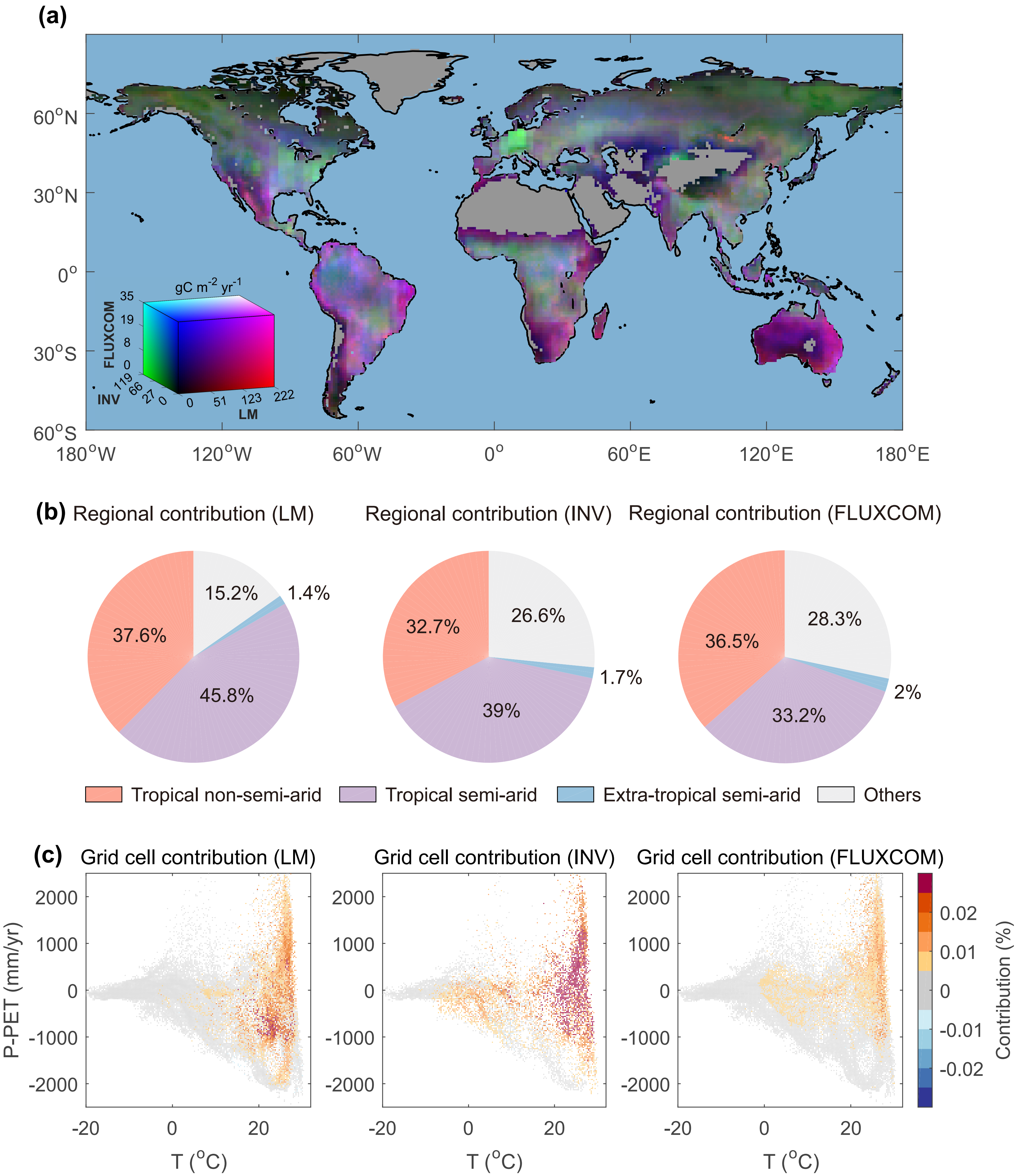

(a)
gC m-2 yr-1
FLUXCOM
INV
LM
60°N
30°N
0°
30°S
60°S
180°W
120°W
60°W
0°
60°E
120°E
180°E
(b) Regional contribution (LM)
Regional contribution (INV)
Regional contribution (FLUXCOM)
37.6%
15.2%
1.4%
45.8%
32.7%
26.6%
1.7%
39%
36.5%
28.3%
2%
33.2%
Tropical non-semi-arid
Tropical semi-arid
Extra-tropical semi-arid
Others
(c) Grid cell contribution (LM)
Grid cell contribution (INV)
Grid cell contribution (FLUXCOM)
P-PET (mm/yr)
T (°C)
Contribution (%)

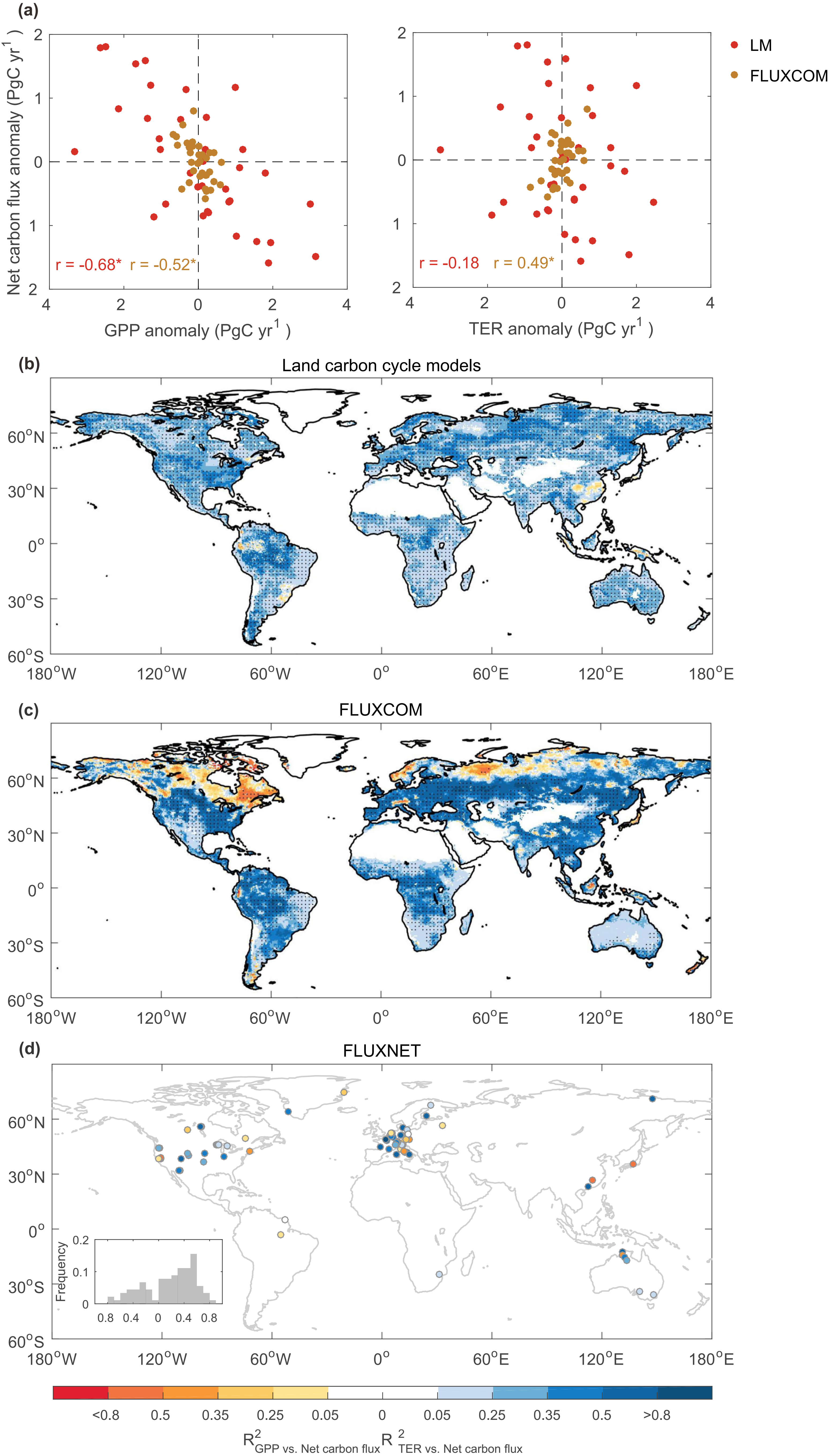
(a)
Net carbon flux anomaly (PgC yr1)
GPP anomaly (PgC yr1)
r = -0.68*
r = -0.52*
TER anomaly (PgC yr1)
r = -0.18
r = 0.49*
LM
FLUXCOM
(b)
Land carbon cycle models
(c)
FLUXCOM
(d)
FLUXNET
Frequency
60°N
30°N
0°
30°S
60°S
180°W
120°W
60°W
0°
60°E
120°E
180°E
<0.8
0.5
0.35
0.25
0.05
0
0.05
0.25
0.35
0.5
>0.8
R2 GPP vs. Net carbon flux
R 2 TER vs. Net carbon flux

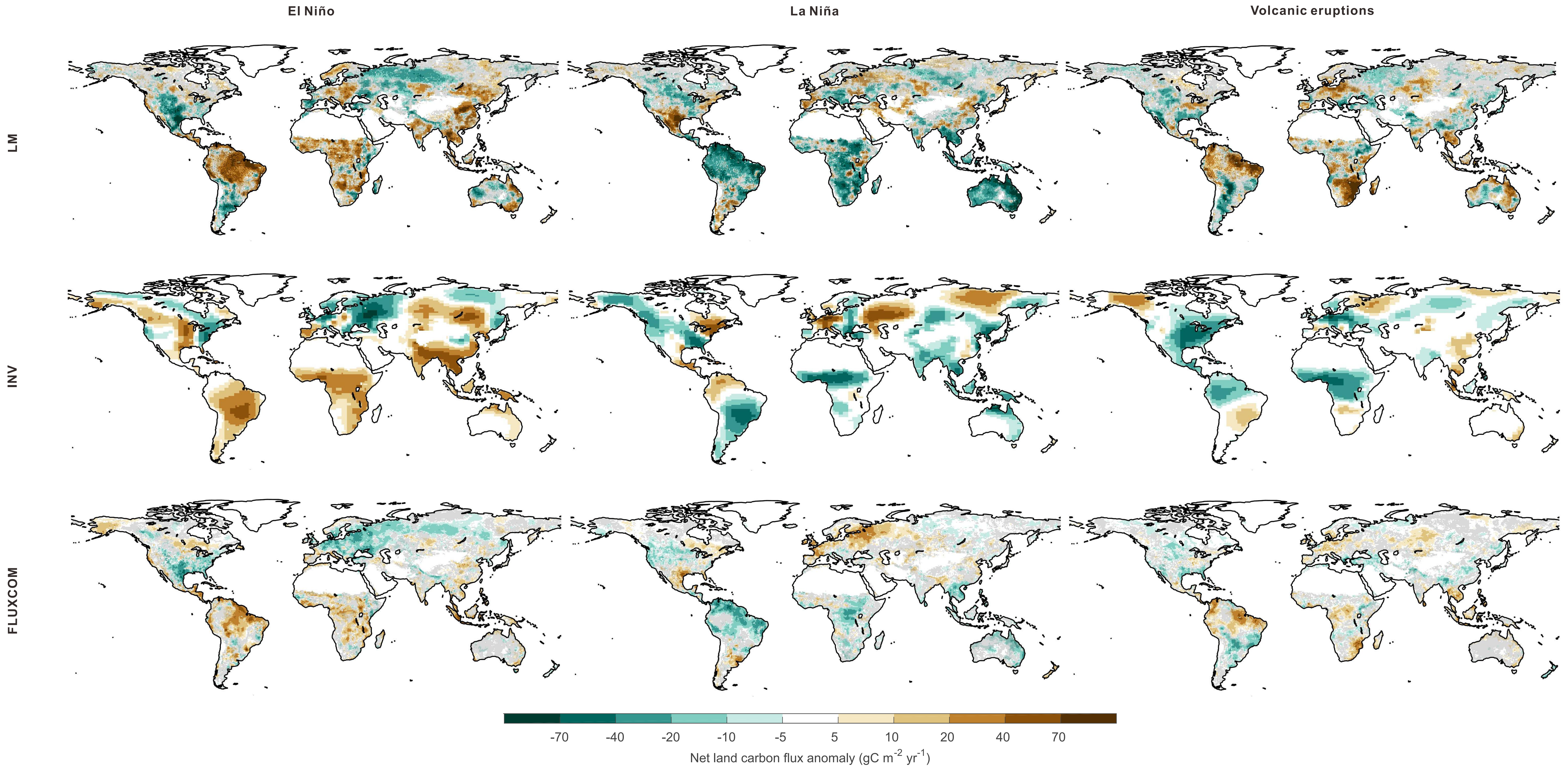
El Niño
La Niña
Volcanic eruptions
LM
INV
FLUXCOM
-70
-40
-20
-10
-5
5
10
20
40
70
Net land carbon flux anomaly (gC m^{-2} yr^{-1})

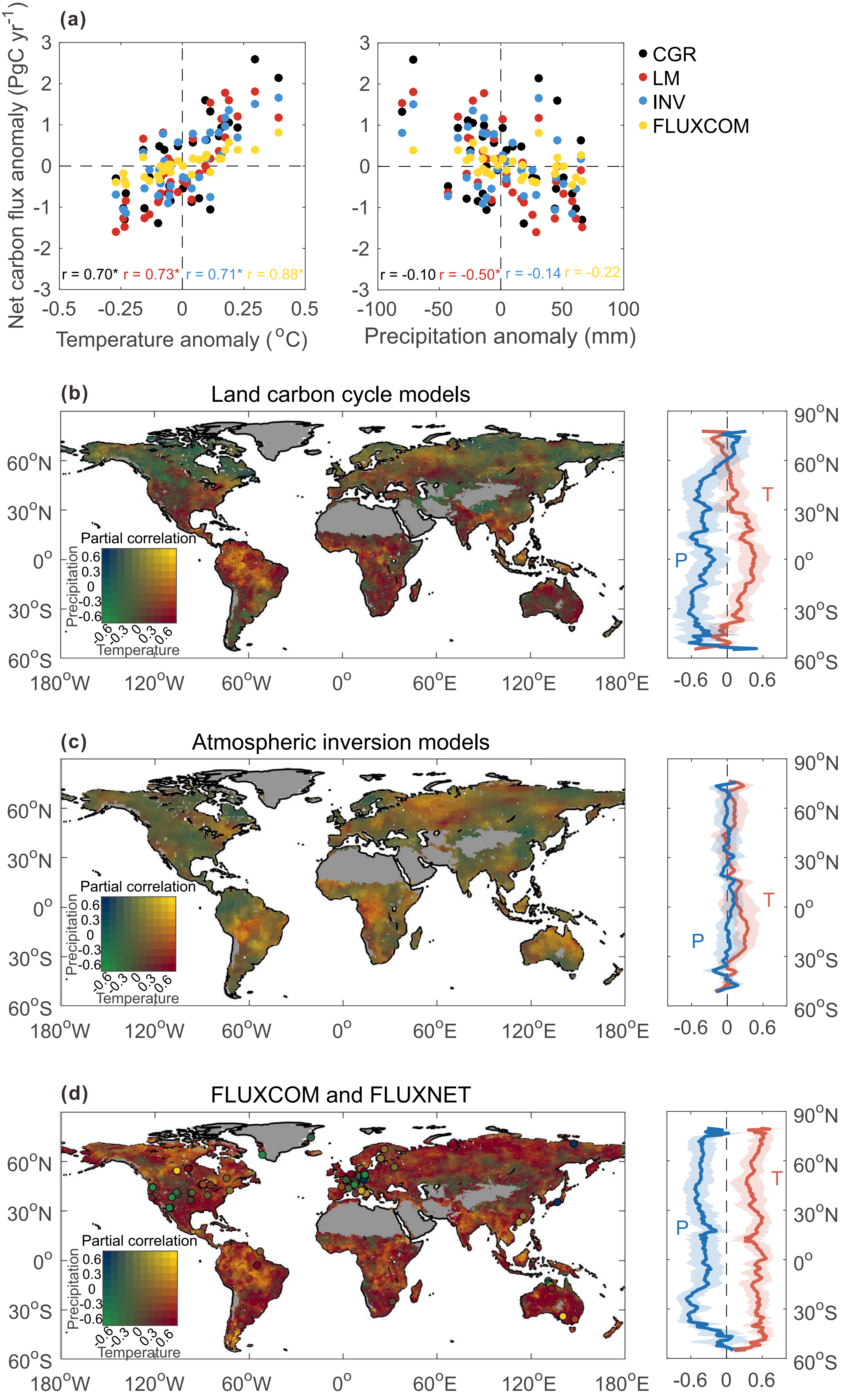

(a)
Net carbon flux anomaly (PgC yr^{-1})
Temperature anomaly (^{o}C)
Precipitation anomaly (mm)
r = 0.70* r = 0.73* r = 0.71* r = 0.88*
r = -0.10 r = -0.50* r = -0.14 r = -0.22
CGR
LM
INV
FLUXCOM
(b) Land carbon cycle models
(c) Atmospheric inversion models
(d) FLUXCOM and FLUXNET
Partial correlation
Precipitation
Temperature
P
T

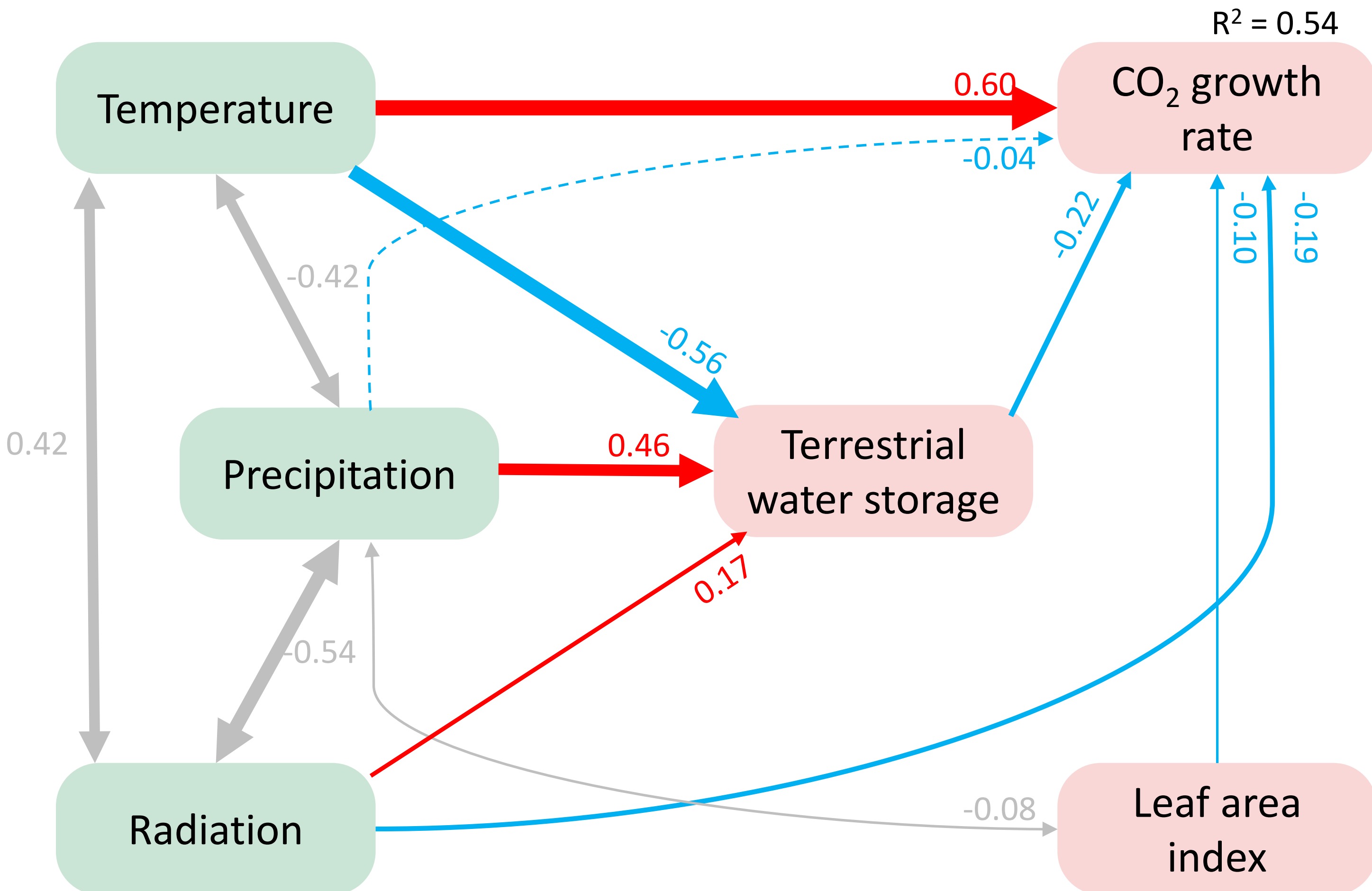

χ^2/dF = 1.3, p = 0.26, AGFI = 0.97, RMSEA =0.03

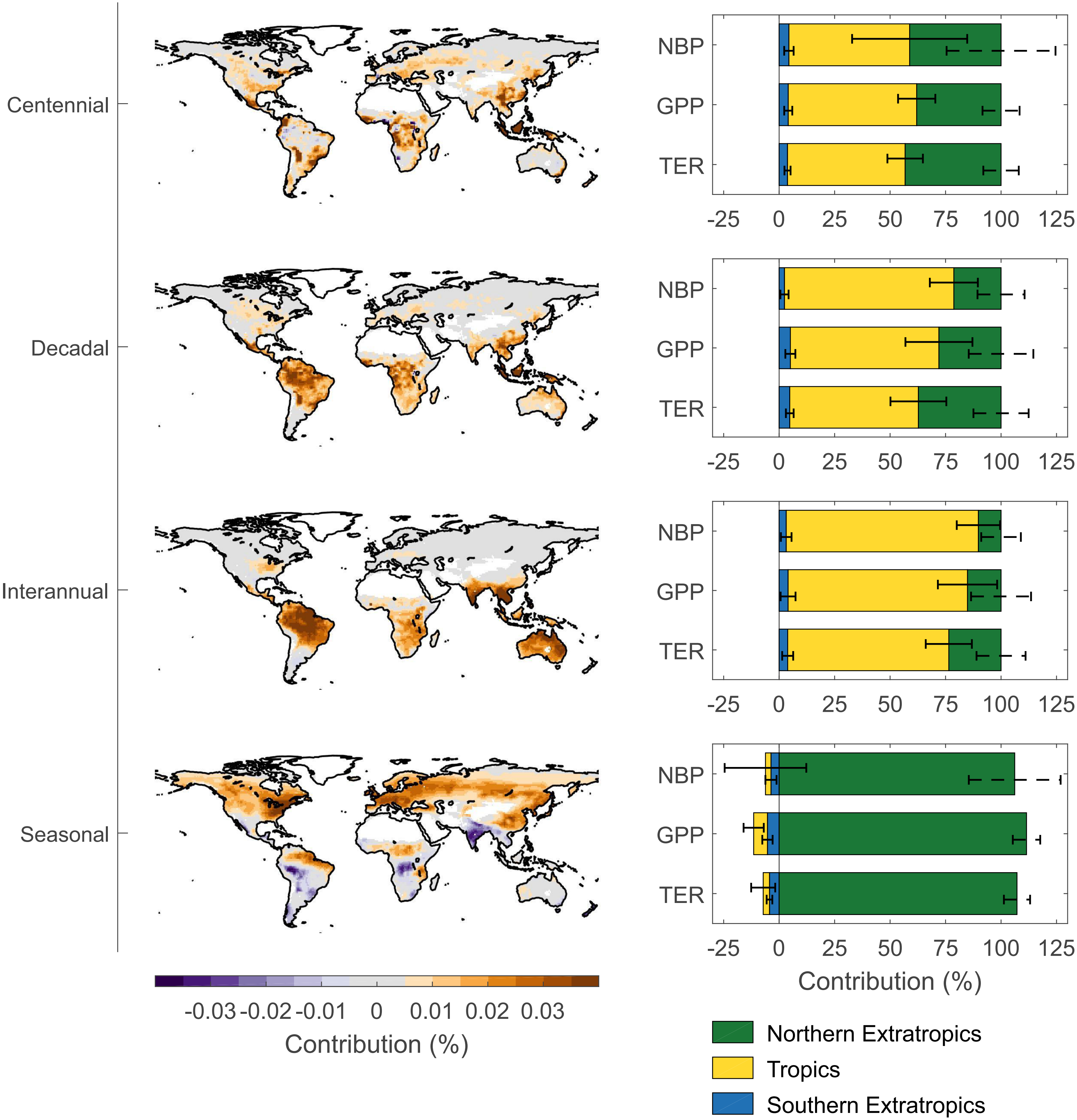

Centennial
Decadal
Interannual
Seasonal
NBP
GPP
TER
-25
0
25
50
75
100
125
Contribution (%)
-0.03
-0.02
-0.01
0
0.01
0.02
0.03
Contribution (%)
Northern Extratropics
Tropics
Southern Extratropics

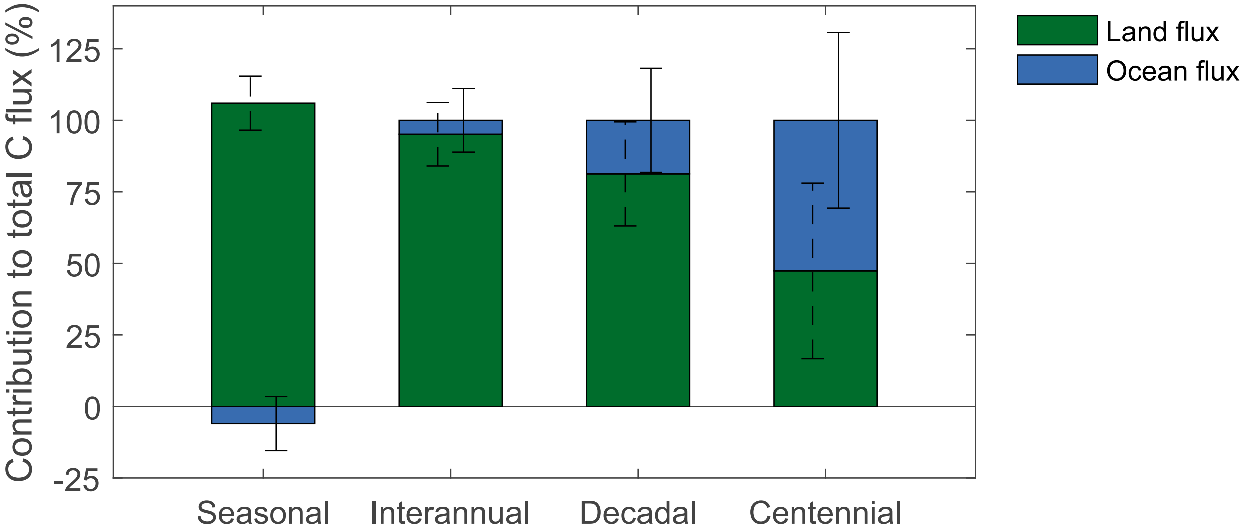

Contribution to total C flux (%)
125
100
75
50
25
0
-25
Seasonal
Interannual
Decadal
Centennial
Land flux
Ocean flux